Atmos. Chem. Phys. Discuss., doi:10.5194/acp-2016-385, 2016
Manuscript under review for journal Atmos. Chem. Phys.
Published: 20 May 2016

Atmospheric Chemistry and Physics Discussions

An observationally-constrained estimate of global dust aerosol optical depth

David A. Ridley[1], Colette L. Heald[1], Jasper F. Kok[2], Chun Zhao[3]

[1]Civil and Environmental Engineering, Massachusetts Institute of Technology
[2]Department of Atmospheric and Oceanic Sciences, UCLA
[3]Atmospheric Sciences and Global Change Division, Pacific Northwest National Lab, Richland, WA 99352

Correspondence to: David A. Ridley (daridley@mit.edu)

Abstract. Global climate and chemistry models routinely simulate dust emission, transport, and deposition to provide estimates of the role dust plays in climate and ecosystems. However, differences between these model simulations are substantial, with estimates of global dust aerosol optical depth (AOD) that vary by over a factor of 5. Here we develop an observationally-based estimate of the global dust AOD, using multiple satellite platforms, in-situ AOD observations and four state-of-the-science global models over 2004 - 2008. We estimate that the global dust AOD at 550 nm is 0.033 ± 0.006 (2σ), higher than the AeroCom model median (0.023) and substantially narrowing the uncertainty. The methodology used provides regional, seasonal dust AOD and the associated statistical uncertainty for key dust regions around the globe with which model dust schemes can be evaluated. Exploring the regional and seasonal differences in dust AOD between our observationally-based estimate and the four models in this study, we find that emissions in Africa are often overrepresented at the expense of Asian and Middle-Eastern emissions, and that dust removal appears to be too rapid in most models.

1 Introduction

Mineral dust is a key component of aerosol, affecting climate through interaction with radiation, clouds and snowpack, human health through contribution to particulate matter ($PM_{2.5}$), and ecosystem health through nutrient transport and deposition. The direct radiative effect (DRE) of dust contributes ~30% of the total aerosol global mean DRE (Heald et al., 2014); however, there is significant uncertainty in the radiative forcing of dust, estimated to be anywhere between -0.3 and +0.1 Wm^{-2} (Boucher et al., 2013), owing to large uncertainties in the anthropogenically-driven changes in dust (Ginoux et al., 2012; Heald and Spracklen, 2015) and the particle morphology and absorption properties (e.g. Balkanski et al., 2007; Mishra et al., 2008). Dust concentrations are often highest in remote regions that are sparsely-monitored, leading to further uncertainty on the atmospheric burden and the associated radiative effects. Dust aerosol can be transported far downwind of desert source regions, having a significant impact on the surface $PM_{2.5}$ thousands of kilometers downwind (Prospero, 2007; Prospero et al., 2014; Zhang et al., 2013). This poses a significant health concern through cases of premature mortality from respiratory and cardiovascular disease that are attributed to aerosol exposure (Lim et al., 2012). Studies attempting to quantify the global premature mortality from aerosol exposure (e.g. van Donkelaar et al., 2006; Evans et al., 2013) highlight the strong contribution

Atmos. Chem. Phys. Discuss., doi:10.5194/acp-2016-385, 2016
Manuscript under review for journal Atmos. Chem. Phys.
Published: 20 May 2016

Atmospheric Chemistry and Physics Discussions

of dust to $PM_{2.5}$ across large regions of Africa, Asia and the Middle East. Because of the lack of surface monitoring in dust influenced regions, those studies rely on satellite observations of aerosol optical depth (AOD), a measure of the column-integrated aerosol that is critical for understanding the radiative effect. Relating the AOD to surface $PM_{2.5}$ requires information on the vertical distribution and aerosol speciation, generally obtained from models, which can introduce considerable uncertainty (Ford and Heald, 2015). Limited observations of global dust aerosol hinder our ability to estimate the full extent of the climate and air quality impacts of mineral dust.

To simulate dust aerosol models must be able to predict the vertical dust flux from suitable regions and represent the evolution of the particle size distribution while the dust is transported and deposited out of the atmosphere. The AeroCom project, an intercomparison and evaluation of different aerosol models, provides a detailed evaluation of dust aerosol simulation from multiple models (Huneeus et al., 2011). There is a considerable spread in global dust AOD estimates from models ranging from 0.010 to 0.053 with an AeroCom model median of 0.023 and standard deviation of 0.011. The uncertainty in the AOD highlights the underlying uncertainties in emissions, size distributions, lifetime, and optical properties. Even over the well-studied, most productive dust region of West Africa, climate models struggle to represent dust emission and their year-to-year changes (Evan et al., 2014). An observationally-constrained estimate of dust AOD can provide a suitable metric to holistically evaluate model dust emission, transport, and deposition, thereby helping constrain both the direct radiative effect and the role of dust in adverse health effects from exposure to $PM_{2.5}$. Here we derive such a metric, with consideration for the sources of uncertainty, and use it to highlight seasons and regions in which current global models deviate from the observations.

2 Data Description

In this study we make use of AOD retrievals from three satellite instruments as well as surface-based sun photometers in combination with four global aerosol models that provide information on non-dust aerosol AOD and the spatial distribution of dust aerosol. We use observational data and model simulations over the 5-year period between 2004 and 2008, except when calculating biases between satellite and surface-based observations, for which we leverage a longer dataset between 2002 and 2012. Below we give a brief description of each instrument and model, and the products used.

2.1 Moderate Resolution Imaging Spectroradiometer (MODIS)

Two MODIS instruments are in sun-synchronous orbit aboard the Terra and Aqua platforms, making equatorial overpasses at 10.30am and 2.30pm local time (LT), respectively. Radiance measurements are made across 36 bands between 0.4 and 14 microns, with 7 channels used to retrieve the AOD at 550 nm. The wide swath (2330 km) allows almost daily coverage of the globe by both instruments at a native resolution of 500 m at nadir (2 km at swath edge), for the aerosol-relevant bands, with AOD reported at approximately 10 km x 10 km resolution (Level-2 product). The Collection 6 MODIS data includes a merged AOD product that combines retrievals over ocean, vegetated land surface (Dark Target), and bright land surface (Deep Blue) to maximize global coverage. The retrieved AOD (τ) is estimated to be accurate to $0.03 \pm 0.05\tau$ over ocean (Remer et al.,

Atmos. Chem. Phys. Discuss., doi:10.5194/acp-2016-385, 2016
Manuscript under review for journal Atmos. Chem. Phys.
Published: 20 May 2016

Atmospheric Chemistry and Physics Discussions

2005), 0.05 ± 0.15τ over dark land surfaces (Levy et al., 2010) and 0.05 ± 0.20τ over bright surfaces (Hsu et al., 2006; Sayer et al., 2013). The Level-2 AOD retrievals are aggregated on a daily basis onto a 1° x 1° grid (Level-3) with statistics, including cloud fraction and standard deviation. Throughout this study we use the Level-3 product.

2.2 Multi-angle Imaging Spectro-Radiometer (MISR)

The MISR instrument, aboard the Terra satellite platform, measures radiance over 9 camera angles with an equatorial overpass at 10.30am LT. The relatively narrow swath width (400 km) results in global coverage every 9 days, compared with 1 - 2 days by MODIS. MISR provides AOD at four wavelengths (446nm, 558nm, 672nm, 867nm) with about three-quarters of retrievals falling within 0.05 or 0.20τ of AERONET observations and reliable retrieval over bright desert surfaces (Kahn et al., 2010; Martonchik et al., 1998, 2004). In this study we use the Level-3 daily 0.5° x 0.5° resolution gridded AOD product.

2.3 Aerosol Robotic Network (AERONET)

AERONET consists of a global network of Cimel Electronique CE-318 sun photometers, which reports AOD with a high degree of accuracy leading to estimated errors of ~0.01 - 0.02 (Eck et al., 1999; Holben et al., 1998). Direct sun measurements are made every 15 minutes at 340, 380, 440, 500, 675, 870, 940 and 1020 nm and AOD is retrieved at all but the 940 nm channel, which is used to provide total column water vapor. We use Level 2.0 data that has been screened for clouds (Smirnov et al., 2000) and use the angstrom exponent (Ångström, 1964) between the AOD at 440 and at 870 nm to distinguish AOD dominated by coarse aerosol (e.g. O'Neill et al., 2001; Reid et al., 1999).

2.4 GEOS-Chem

We use the GEOS-Chem global chemical transport model (v9-01-01; http://www.geos-chem.org) to simulate the coupled oxidant-aerosol chemistry of the troposphere at a resolution of 2.5° by 2.0° over 47 vertical levels following the specifications used in (Heald et al., 2014). The oxidant-aerosol simulation includes H_2SO_4-HNO_3-NH_3 aerosol thermodynamics described by ISORROPIA II (Fountoukis and Nenes, 2007) and coupled with an O_3-NO_x-hydrocarbon chemical mechanism (Park et al., 2004, 2006). The aerosol simulation also includes carbonaceous aerosols (Park et al., 2003; Pye et al., 2010; Pye and Seinfeld, 2010), mineral dust (Fairlie et al., 2007; Ridley et al., 2012), and sea salt (Alexander et al., 2005). Aerosol mass is transported in 4 size bins (0.1–1.0, 1.0–1.8, 1.8–3.0, and 3.0–6.0 μm radius) for dust, two for sea-salt and one for each of the other species. The model is driven by assimilated meteorology from the NASA Modern-Era Retrospective analysis for Research and Applications (MERRA), which provides winds, precipitation, could cover etc. at 1-hourly and 3-hourly temporal resolution. Dust emissions are generated using the DEAD scheme (Zender, 2003) with the GOCART source function (Ginoux et al., 2001; Prospero et al., 2002) and a fixed soil clay fraction of 0.2. We follow Ridley et al. (2013) by using a probability distribution of sub-grid scale winds, generated from 0.5° x 0.67° MERRA 10-m winds, rather than the average wind speed when calculating dust uplift. Biomass burning emissions are provided by the Global Fire Emissions Database version 3 (GFEDv3; van der Werf et al., 2010). Anthropogenic emissions are provided by the Emissions Database for Global Atmospheric Research (EDGAR)

Atmos. Chem. Phys. Discuss., doi:10.5194/acp-2016-385, 2016
Manuscript under review for journal Atmos. Chem. Phys.
Published: 20 May 2016

v3.2 inventory (Olivier, 2001) for SO_x, NO_x, and CO which is superseded by the National Emissions Inventory (NEI99; http://www.epa.gov/ttn/chief/net/1999inventory.html) over the United States and Streets et al. (2003, 2006) over Asia (van Donkelaar et al., 2008). Sea salt emissions follow Gong (2003) with added dependence on sea surface temperature (Jaeglé et al., 2011). AOD at 550nm is calculated online assuming lognormal size distributions of externally mixed aerosols and is a function of the local relative humidity to account for hygroscopic growth (Martin et al., 2003). Aerosol optical properties are based on the Global Aerosol Data Set (GADS) (Hess et al., 1998a) with modifications to the size distribution based on field observations (Drury et al., 2010; Jaeglé et al., 2011) and improvements to the UV/visible refractive indices of dust (Sinyuk et al., 2003).

2.5 CESM

The Community Earth System Model (CESM), version 1.1 (Hurrell, 2013), is used in this study following the specifications described in (Kok et al., 2014b). The atmospheric component of the model, the Community Atmospheric Model version 4 (CAM4), is run at 2.5° x 1.9° resolution and is driven by ERA-Interim reanalysis meteorology (Dee et al., 2011) with free-running dynamics. CAM4 simulates aerosol as bulk species from the Model for OZone And Related chemical Tracers (MOZART) chemistry package (Lamarque et al., 2012), including sulfate, ammonium, ammonium nitrate, black carbon, organic carbon and secondary organic aerosol. Emissions of these species are prescribed by the AeroCom specifications (Neale et al., 2010). Sea salt is emitted and transported in four size bins and is calculated from 10 m wind speed (Mahowald et al., 2006). Dust emission in the Community Land Module version 4 (CLM4) is traditionally based on the DEAD dust scheme (Zender, 2003) with some minor modifications (Mahowald et al., 2006, 2010). Here we use an updated version of the dust emission model that generates a vertical dust flux with no prescribed source function, and that accounts for the exponential increase in dust flux with increasing soil erodibility (Kok et al., 2014a, 2014b). Dust is emitted into four size bins (0.1–1.0, 1.0–2.5, 2.5–5.0, and 5.0–10 μm diameter), and the fraction emitted into each bin is independent of wind speed, as shown by measurements (Kok, 2011b), and distributed following brittle fragmentation theory (Kok, 2011a). All aerosols are assumed externally mixed and aerosol optical properties are based on GADS (Hess et al., 1998a) with improvements to the dust optical properties described in (Albani et al., 2014). Assumed size distributions for bulk aerosol can be found in Emmons et al. (2010).

2.6 WRF-Chem

The quasi-global configuration of the WRF-Chem (version 3.5.1) model is used in this study, described in detail in Hu et al. (2016). The simulation uses the MOSAIC (Model for Simulation Aerosol Interactions and Chemistry) aerosol module (Zaveri et al., 2008) with the CBM-Z (carbon bond mechanism) photochemical mechanism (Zaveri and Peters, 1999). A sectional approach is used to represent aerosol size distributions with eight discrete size bins and all major aerosol components including sulfate (SO_4^{-2}), nitrate (NO_3^-), ammonium (NH_4^+), black carbon (BC), organic matter (OM), sea-salt, methanesulfonic acid, and mineral dust are simulated. The MOSAIC aerosol scheme includes physical and chemical processes of nucleation, condensation, coagulation, aqueous phase chemistry, and water uptake by aerosols. The model is run at a resolution of 1° x

Atmos. Chem. Phys. Discuss., doi:10.5194/acp-2016-385, 2016
Manuscript under review for journal Atmos. Chem. Phys.
Published: 20 May 2016

1° (between 180° W-180° E and 67.5° S-77.5° N) with 35 vertical layers up to 50hPa (Hu et al., 2016). The modeled u and v wind components and temperature in the free atmosphere above the planetary boundary layer are nudged towards NCEP/FNL reanalyses on 6-hourly time steps (Stauffer and Seaman, 1990). Biomass burning emissions are derived from GFEDv3. Anthropogenic emissions are provided by the REanalysis of the TROpospheric (RETRO) chemical composition inventories (http://retro.enes.org/index.shtml) except over East Asia, where emissions are taken from the inventory developed for the INTEX-B mission in 2006 (Zhang et al., 2009), updated with SO_2 and carbonaceous emissions from Lu et al. (2011), and the United States, where the National Emissions Inventory (NEI) for 2005 are used. Sea salt emissions are based on (Gong, 2003), with added emission dependence on sea surface temperature (Jaeglé et al., 2011). Dust emission fluxes are calculated with the GOCART dust emissions scheme (Ginoux et al., 2001) and partitioned into the MOSAIC size bins based on brittle fragment theory (Kok, 2011a). Aerosol optical properties are computed as a function of wavelength for each model grid box. Aerosols are assumed internally mixed (a volumetric mean refractive index) in each bin. The Optical Properties of Aerosols and Clouds (OPAC) dataset (Hess et al., 1998b) is used for the shortwave (SW) and longwave (LW) refractive indices of aerosols, except that a constant value of 1.53 + 0.003i is used for the SW refractive index of dust following Zhao et al. (2010, 2011). A detailed description of the aerosol optical properties calculated in WRF-Chem can be found in (Fast et al., 2006) and (Barnard et al., 2010). The optical properties and direct radiative forcing of individual aerosol species in the atmosphere are diagnosed following the methodology described in Zhao et al. (2013).

2.7 MERRAero

The NASA Global Modeling and Assimilation Office (GMAO) GEOS-5 Earth system model can be run in a configuration that assimilates meteorological and aerosol properties retrieved from NASA Earth observing satellite platforms (Rienecker et al., 2011). The resulting aerosol simulation is termed MERRAero. The simulation is run at a resolution of 0.5° x 0.625° providing speciated AOD with 3-hourly temporal resolution. The aerosol processes are based on the Goddard Chemistry, Aerosol, Radiation and Transport model (GOCART; Chin et al., 2002) with coupling of chemistry and climate (Colarco et al., 2010). Dust, sulfate, organic carbon, black carbon and sea salt are simulated as external mixtures. Dust aerosol is partitioned into 8 size bins between 0.1 and 10 µm particle radius, and sea salt aerosol is partitioned into 5 size bins between 0.03 and 10 µm dry radius; all other aerosol is transported in a single size bin per species. Emissions of fossil fuels and biofuel follow the GOCART model (Chin et al., 2002) with updates in the U.S. following Park et al. (2003). SO_2 emissions are from the EDGAR-4.1 inventory with altered injection profiles (Buchard et al., 2014) and biomass burning emissions are supplied from the NASA Quick Fire Emission Dataset (QFED) Version 2.1. Sea salt aerosol production follows Gong (2003) with added dependence on sea surface temperature (Jaeglé et al., 2011). The aerosol optical properties follow GADS, but with modifications to reduce the absorption of dust at short wavelengths (Sinyuk et al., 2003), and extinction is calculated following Mie theory assuming spherical particles (Colarco et al., 2010). MERRAero differs from the other three models used in that the model assimilates AOD information from the MODIS instruments. The assimilation process is explained in detail in Buchard et al. (2016), here we give a brief description. The MODIS reflectances are cloud screened and converted to AOD using a neural net framework.

Atmos. Chem. Phys. Discuss., doi:10.5194/acp-2016-385, 2016
Manuscript under review for journal Atmos. Chem. Phys.
Published: 20 May 2016

The error covariance between the 2D MODIS AOD and the model AOD is used to generate 3D aerosol mass increments. Using a Local Displacement Ensemble (LDE) methodology, ensembles of isotropic displacements in aerosol mass around a central grid box are weighted based upon the reduction in the error. Different aerosol species can be perturbed in each vertical layer, e.g. to allow a plume to be shifted to better match the MODIS AOD, and therefore aerosol mass can vary independently for each species.

3 Methodology

3.1 Derivation of dust AOD

Our aim is to provide seasonal dust AOD estimates, both global and regional, that are as independent from modeled dust estimates as possible. The methodology and development of associated uncertainty estimates is described in detail below, but the general methodology is as follows: We rely primarily on satellite retrievals of AOD, with correction by dust-dominated AERONET AOD retrievals. Model seasonal estimates of AOD from non-dust species are used to extract the dust AOD in regions that are identified as contributing significantly to the global dust AOD. These regions are defined such that they account for the majority of dust AOD, based on model estimates, and are shown in Figure 1. Finally, model dust AOD is used to relate the regional dust AOD to the global dust AOD, providing global seasonal dust AOD estimates between 2004 and 2008, to give the multi-year seasonal averages.

Daily AOD data from MISR and both MODIS instruments (Aqua and Terra) are aggregated onto a 2° x 2.5° grid and averaged over 3-month periods to increase coverage and provide a consistent grid between model and observations. A bootstrapping method (Efron and Gong, 1983) is used to estimate the random uncertainty in the seasonally-averaged AOD due to sampling uncertainty within each grid box. This is achieved by randomly sampling (with replacement) the grid box daily AOD n times, where n is the number of days with a retrieval in that 3-month period, to provide a probability distribution. We find that a normal distribution is a good approximation to the resulting seasonal AOD uncertainty distribution, so we retain the mean and standard deviation of this distribution as the mean and uncertainty on the AOD for each grid box.

Although the bootstrapping method quantifies the random error in each grid box' seasonal AOD, it does not quantify or correct the systematic error (bias) in the AOD. Therefore, we use AERONET AOD as ground-truth to apply a bias correction to the satellite-retrieved AOD, with a focus on dust influenced regions. AERONET hourly AOD (interpolated to 550nm) is used to produce a morning (10am – noon, LT) and afternoon (1pm – 3pm, LT) average to compare with daily retrievals from aboard the Terra and Aqua satellites, respectively. We compare these at the native satellite retrieval resolution and choose a two-hour window to both cover the approximate range of the overpass times and to maximize the number of coincident AERONET and satellite AOD retrievals. Note that this analysis is performed at the location of all the AERONET sites in Figure 1, not solely those within the 15 dust-dominated regions we have identified in Figure 1. To better isolate cases in which dust influence likely dominates, we only consider AERONET retrievals when the angstrom exponent (AE) is less than 0.4 (e.g. Muller et al., 2003; Prasad and Singh, 2007). This removes observations when the AOD is dominated by fine mode aerosols that may skew

Atmos. Chem. Phys. Discuss., doi:10.5194/acp-2016-385, 2016
Manuscript under review for journal Atmos. Chem. Phys.
Published: 20 May 2016

Atmospheric Chemistry and Physics Discussions

the bias correction to regions strongly affected by anthropogenic aerosol and not dust (see Figure 1 for the location of the AERONET sites). Statistics of the bias and linear regression between AERONET and satellite retrievals are calculated for the seasonal (3-monthly) climatology between 2002 and 2012 and used to scale the slope and y-intercept of the satellite AOD to match that of the co-located AERONET data (see Figure 2). Although 2004 – 2008 is the man period of study in this research we use 11 years of AERONET and satellite retrievals to maximize the amount of data and better characterize the biases.

On average across all sites, both MODIS instruments show very little mean annual bias in AOD relative to AERONET retrievals with AE<0.4 (+1% for Terra; -2% for Aqua; see Figure 2), although there is considerable variability on a day-to-day basis. The correlation between MODIS and AERONET is good (r=0.83 for both), and similar for MISR and AERONET (r=0.84). MISR is biased high relative to AERONET (+7%), owing primarily to retrievals when AOD<0.5, but also exhibits a low bias for AOD>1.0, consistent with previous comparisons, e.g. Moon et al. (2015). There is no clear seasonality in the bias between the satellite and AERONET AOD for any of the instruments. Initially, we implemented a site-dependent bias correction using the spatial covariance of the AOD to propagate the bias correction away from AERONET sites; however, strong bias corrections that could not be confirmed often propagated from polluted regions into remote locations. Therefore, a single correction per satellite instrument is used globally owing to the sparse AERONET data in the regions most affected by dust. The bias correction has a negligible impact on the average global dust AOD (-1%), but causes a 9% decrease in the uncertainty about that average as the satellite AOD retrievals are brought into closer alignment (see Table 1).

Although dust aerosol is often the main contributor to the AOD in the regions shown in Figure 1, other aerosol species can make a significant contribution and need to be accounted for to extract dust AOD from the satellite retrievals of AOD. We use GEOS-Chem, CESM, WRF-Chem and MERRAERO to provide non-dust AOD; multiple models provide an estimate of the variability in the non-dust portion of the AOD resulting from uncertainty in aerosol emissions and formation mechanisms. Anthropogenic aerosol is generally well characterized by global models, especially on seasonal timescales, and have been regularly evaluated against observations, particularly in the Northern Hemisphere (e.g. Hu et al., 2016; Leibensperger et al., 2012; Liu et al., 2012; Mann et al., 2014). Biomass burning aerosol concentrations are inherently uncertain because of the challenges in determining burned area and emissions factors (French et al., 2004; van der Werf et al., 2006). Despite considerable evaluation against observations the resulting biomass burning AOD is sometimes underrepresented (Matichuk et al., 2007; Reddington et al., 2016); therefore, we treat regions affected by biomass burning emissions with caution. In the regions analyzed here the AOD is predominantly driven by dust aerosol, limiting the influence of the model non-dust AOD. Exceptions to this are in South America, South Africa, and Australia, that have a minimal impact on the global dust AOD, and the Gulf of Guinea, where significant biomass burning aerosol is present (we consider results with and without these regions, see Table 1). In addition, most regions considered in this study are inland and therefore sea salt aerosol will have a limited impact. Figure 3 displays the climatology of non-dust AOD and dust AOD for each model used, averaged over 2004 - 2008.

For each 2° x 2.5° grid box, *i*, within the 15 regions we apply the AERONET-derived bias correction, α, to the seasonal satellite AOD, τ^{obs}, and subtract the model non-dust AOD, τ_{nd}^{model}, to provide an estimate of the regional dust AOD, τ_d^{reg} (Eqn. 1). We allow negative values of τ_d^{reg} so as not to introduce a positive bias. The uncertainty distribution for each of these three

Atmos. Chem. Phys. Discuss., doi:10.5194/acp-2016-385, 2016
Manuscript under review for journal Atmos. Chem. Phys.
Published: 20 May 2016

Atmospheric Chemistry and Physics Discussions

variables (bias correction, satellite AOD, and model non-dust AOD) is sampled and the average dust AOD is calculated for each region. This process is repeated multiple times to yield a stable distribution of seasonal dust AOD (100 times is sufficient for a robust average) for each of the regions between 2004 and 2008. For a single iteration of the dust AOD calculation we use the same random sampling (sampling the same number of sigma from the mean) for all grid boxes, thereby assuming the worst case scenario that the uncertainty is correlated spatially. If we use a different sampling of the uncertainty distribution for each grid box, the uncertainty on the global dust AOD drops by approximately a factor of 8.

$$\tau_d^{reg} = \frac{1}{N}\sum_{i}^{N} \alpha\tau_i^{obs} - \tau_{nd,i}^{model} \quad (1)$$

The regional dust AOD, τ_d^{reg}, for the 15 regions is weighted by surface area, A^{reg}, summed, and scaled by the surface area of the Earth, A_E, to give the total regional contribution to the global dust AOD (Eqn. 2). To obtain the globally-averaged dust AOD, τ_d^{glob}, we calculate the ratio, β, between the modeled dust AOD across all regions and the modeled global dust AOD (Eqn. 3).

$$\tau_d^{glob} = \beta \frac{1}{A_E}\sum_r^{N^{reg}} A^{reg}\tau_d^{reg}, \quad (2)$$

$$\beta = \frac{\tau_d^{glob,model}}{\frac{1}{A_E}\sum_r^{N^{reg}} A^{reg}\tau_d^{reg,model}} \quad (3)$$

This allows the satellite estimate within the regions to be scaled to a global dust AOD estimate. This is the only element of our analysis that relies upon simulated dust AOD. The 15 regions account for between 83% and 95% of the global dust AOD, depending on the model, so the model influence is limited and using multiple models provides an estimate of the uncertainty this introduces into our analysis (see Table 1). This process is repeated for different combinations of satellite instrument and model estimates for non-dust and regional-to-global scaling, leading to 48 realizations, 16 per satellite instrument, each with an uncertainty estimate. We use the kernel density estimation method (Silverman, 1986) with a Gaussian kernel and standard smoothing to determine a probability density function for the global dust AOD.

4 Results

4.1 The observationally-constrained global dust AOD

Figure 4 summarizes our observationally-constrained global dust AOD estimate, averaged over the 2004 – 2008 period. The global dust AOD for the AeroCom models in Huneeus et al. (2011) is also displayed in Figure 4 with the associated probability density function generated using the kernel density estimation method. Our observational estimate of the global dust AOD is centered around an average of 0.033 ± 0.006 (2σ), much more narrowly constrained than the AeroCom estimate of 0.028 ± 0.011. All but 3 of the 48 realizations (94%) fall above the AeroCom model mean global dust AOD; however, the broadness of the AeroCom model distribution implies that a global dust AOD greater than 0.035 would be required for statistically

Atmos. Chem. Phys. Discuss., doi:10.5194/acp-2016-385, 2016
Manuscript under review for journal Atmos. Chem. Phys.
Published: 20 May 2016

significant disagreement at the 95% confidence level (i.e. $p < 0.05$; in this case $p = 0.18$). Relative to the dust AOD from the four models used in this study (see Figure 3), two lie within 1σ of the observational estimate and two below. The average global dust AOD estimates from each satellite instrument are remarkably similar (MODIS Aqua: 0.033, MODIS Terra: 0.033, MISR: 0.032). This is partially owing to the AERONET bias correction; however, even without bias correction the global dust AOD estimates are similar (MODIS Aqua: 0.031, MODIS Terra: 0.033, MISR: 0.035), indicating that the observationally-constrained estimate is not heavily dependent upon the AERONET correction applied. On an annual basis, the observationally-constrained global dust AOD varies between 0.031 and 0.036, with good agreement in the annual dust AOD derived from the three instruments (Figure 5). The dust AOD is similar for years between 2004 and 2006 before increasing in 2007 and peaking in 2008, largely driven by a sharp increase across the Middle East (Yu et al., 2015). The AeroCom model simulations are representative of the year 2000; therefore, some of the difference between the global dust AOD in this study and that from the AeroCom study may derive from the interannual variability. However, the lowest annual global dust AOD, in 2005, still exceeds the AeroCom mean and median. Figure 4 and Figure 5 suggest that dust aerosol is generally underestimated in models, either via mass concentration or the representation of dust extinction. Indeed, a follow-on study indicates that both these factors are underestimated in models (Kok et al., *personal communication, manuscript in preparation*). However, the uncertainty in the observational estimate does encompass several of the models.

4.2 Uncertainties in the observational estimate of global dust AOD

Table 1 summarizes the uncertainties considered in this study, both in terms of potential bias to the global dust AOD and the contribution to the standard deviation of the estimate. The latter is quantified by assessing the reduction in the spread of the global dust AOD PDF when the uncertainty for a factor is omitted. The leading uncertainty arises from the seasonal satellite AOD estimate that is based on a limited number of daily AOD retrievals within a season (±41%). The difference in regional to global dust AOD scaling from models (±19%) and the difference in non-dust AOD from models (±19%) both contribute to the uncertainty. The latter is primarily a consequence of higher non-dust AOD in MERRAero than the other three models and therefore a lower estimate of dust AOD. The regional-to-global scaling factor (β, equation 3) is strongly dependent upon the dust lifetime within the model and ranges from 1.20 to 1.45, a lower scaling factor indicative of less dust far from source and therefore a shorter dust lifetime. The uncertainty from the regional-to-global scaling may not be symmetrical about the mean if the model dust lifetime estimates are biased low, as analysis of dust outflow into the mid-Atlantic suggests (see later discussion). We find that the AERONET bias correction (α, equation 1) plays a minor role in changing the global dust AOD (<1%) and reduces the uncertainty by bringing the different satellite estimates into closer agreement, as expected.

Other factors that are not encompassed by the uncertainty estimate on the global dust AOD are the impact of spatial and temporal sampling biases in the satellite data (e.g. overpass timing and frequency, regions of persistent cloud, high latitudes), cloud filtering of satellite AOD retrievals, and inclusion of the Gulf of Guinea region. These are also included in Table 1 and discussed below.

Atmos. Chem. Phys. Discuss., doi:10.5194/acp-2016-385, 2016
Manuscript under review for journal Atmos. Chem. Phys.
Published: 20 May 2016

Atmospheric Chemistry and Physics Discussions

Satellite retrieval of AOD is only possible in clear sky conditions and at locations that fall within the satellite swath; therefore, the observed dust AOD will not take into account the effect of dust present before or after the satellite overpass, and in the presence of clouds. We assess the impact of this sampling bias by processing the AOD from the 4 models in the same way as the satellite-retrieved AOD, including masking the daily AOD data where no satellite retrieval is available. By comparing the modeled dust AOD with and without masking, we determine that the impact of satellite sampling upon the global dust AOD estimate is minimal, < 1% for the MODIS instruments and +1.3% for MISR. Masking does however increase the uncertainty in the dust AOD estimate by 7% when sampling is based on MODIS and 50% when sampling to the sparser MISR retrievals. The sun-synchronous orbit of the Terra and Aqua satellites results in overpass at similar morning and afternoon local time, respectively, each day. Therefore, a significant daily cycle in the AOD would create a bias in the inferred daily AOD. For all dust-influenced AERONET sites, we compare the 10.00 – 12.00 LT and 14.00 – 16.00 LT AOD to the daily AOD (calculated from all available retrievals within the daytime) between 2002 and 2012. We find that, on the days with AE > 0.4 at the AERONET sites used in this study, the AOD during the morning and the afternoon are closely related to the daily AOD, deviating by < 2% on average. This is in agreement with Smirnov et al., (2002) that found AOD varied diurnally by less than 10% at dust-influenced AERONET sites. When the satellite retrieved AOD is bias corrected to the daily AOD, rather than the AOD at time of overpass (as done here), we find that the dust AOD is 4% lower (see Table 1).

By filtering MODIS daily AOD 1° x 1° retrievals that contain more than 80% cloudy Level-2 pixels we find that the AOD drops considerably in the Mid-Atlantic, Gulf of Guinea and the Arabian Sea (Figure 6). This leads to significantly different estimates for the dust AOD in certain regions (Figure 7). The largest impact is seen in the Mid-Atlantic where the dust AOD declines by 40% on average when filtering for clouds. The models also decrease when the equivalent masking is applied, but only by 20% on average in this region. This suggests that the filtering preferentially removes higher dust AOD cases, but the association of high dust AOD with cloudy regions is stronger in the observations than in the model. Similarly, reductions in dust AOD of up to 30% in winter and spring are produced by cloud filtering in the Gulf of Guinea. In the southern part of the Arabian Peninsula and the Arabian Sea the summertime peak in dust AOD is decreased by 30% by filtering pixels with more than 80% cloud cover. Cloud filtering of Level-2 retrievals is generally considered conservative in Collection 6 and misclassification is more common for thin cirrus than cumulus cloud decks (Levy et al., 2013; Remer et al., 2012). Therefore, removal of large regions in which high dust loading is associated with cumulus and stratus clouds may introduce an erroneous negative bias. It is also possible that high AOD retrieval in cloudy regions is the result of hygroscopicity and 3-D cloud effects (Koren et al., 2007; Marshak et al., 2008; Quaas et al., 2010). Indeed, it has been shown in studies using AERONET that AOD can increase dramatically between clouds and may be mistakenly screened as cloud (Eck et al., 2014). While this is a legitimate AOD enhancement, we cannot expect the global models with >100 km resolution using assimilated meteorology to reproduce enhancements from near-cloud hygroscopic growth or 3-D cloud effects on scattering. The observational-estimate of dust AOD provided in our analysis does not include the extra cloud filtering. We rely on the screening provided as part of the MODIS retrieval, rather than arbitrarily filtering the cloud-cleared product. However, as the enhanced AOD in cloudy regions is unlikely to be captured by models, we have made available the cloud-filtered global dust AOD estimate for all regions.

Atmos. Chem. Phys. Discuss., doi:10.5194/acp-2016-385, 2016
Manuscript under review for journal Atmos. Chem. Phys.
Published: 20 May 2016

The regions defined around the South American, Southern African and Australian deserts and the outflow cover relatively large areas that are only intermittently affected by dust (see Figure 1). This may increase the likelihood of misattribution of non-dust AOD as dust AOD. We find that including those regions in the analysis does not have a significant impact on the global dust AOD, increasing it by <1%, although it causes an 8% increase in the uncertainty. In contrast, including the Gulf of Guinea region increases the dust AOD by +7% and increases the uncertainty by 16%. The dust AOD in the Gulf of Guinea region is consistently higher in the observational estimate than the models owing to a combination of persistent cloud cover, high biomass burning emissions in winter that are not always captured by the models, and a lack of dust towards the equator in the models that may result from too efficient convective wet removal. To prevent an artificially high bias in the global dust AOD, we do not explicitly evaluate the Gulf of Guinea region in our estimates beyond the assessment of uncertainty in Table 1. This region is still accounted for in the global dust AOD via the regional-to-global dust AOD scaling (the 14 remaining regions account for 77% - 87% of the global dust AOD, depending on the model).

4.3 Comparison of modeled and observed regional dust AOD

Model dust emissions are often tuned to a specific annual global emission mass (Fairlie et al., 2007; Huneeus et al., 2011) or scaled to a global AOD inferred from assimilations (Mahowald et al., 2006; Rasch et al., 2001). The annual global dust AOD derived from the models in this study show encouragingly similar interannual variability to the observationally-constrained estimates, even though the global dust AOD is generally underestimated (see Figure 5). However, tuning the models globally will not necessarily produce the right spatial and seasonal distribution. Here we use the observational constraints developed in this study to highlight regional and seasonal discrepancies between models and observations in an effort to isolate potential errors that affect multiple models. We compare the interannual variability globally and the seasonal dust AOD aggregated over broad regions for each of the models with the observational estimates from each satellite instrument (Figure 8a). We also compare the climatological seasonal dust AOD from each model with the range of the observational dust AOD for each region (Figure 8b). We provide regional disaggregation of these results in Figures 9 and 10.

Broadly, in Figure 8 we see that the models, except MERRAero, overestimate the amount of dust AOD over Africa with respect to the satellite estimates. The models generally over-emphasize winter or spring dust at the expense of summer. This is especially the case for GEOS-Chem (highlighted in Ridley et al., 2014; see Fig. S4) and for CESM, and likely a consequence of the lack of convectively-driven dust emissions that will be somewhat alleviated by new parameterizations (e.g. Pantillon et al., 2016). Switching the dust scheme in GEOS-Chem to a new parameterization that does not rely on an explicit source function (Kok et al., 2014a, 2014b) does not alleviate the seasonality issue in Africa, suggesting that the poor performance relative to the other models is likely the result of meteorology rather than the dust parameterization. Isolating the dust AOD in sub-regions we find that the models overestimate dust in the North Africa, West Africa and Atlas Mountain regions, but underestimate the dust AOD in the mid-Atlantic outflow region, although there is significant variability between the four models (see Figure 9 and 10 for the sub-regions).

Atmos. Chem. Phys. Discuss., doi:10.5194/acp-2016-385, 2016
Manuscript under review for journal Atmos. Chem. Phys.
Published: 20 May 2016

In the models, dust AOD over North Africa is greater than observed and dust AOD over the mid-Atlantic is lower than observed (see Figure 9), even when extra cloud filtering of the satellite retrievals is included. This yields a ratio of the dust AOD over Africa to that over the Mid-Atlantic of 3.12 ± 0.31 for the models and 2.42 ± 0.28 based on observations (2.62 ± 0.16 and 1.63 ± 0.08, respectively, with cloud filtering applied). The predominant direction of long-range transport of dust is across the Atlantic; therefore, the models are likely to be removing African dust too rapidly during transport. This is unlikely to be the result of too much dust mass concentrated at large particle sizes that sediment out rapidly, based on comparison between observed and modeled size distributions (Kok, 2011a). Instead, it may stem from the vertical distribution and mixing in the planetary boundary layer that can lead to increased dry and wet removal through proximity to the surface and co-location with precipitating clouds, respectively. Indeed, the choice of boundary layer mixing scheme can have a significant impact on long-range dust transport (Jin et al., 2015). The GEOS-Chem model dust lifetime over the Atlantic was shown to be 25-50% shorter than inferred from MODIS and primarily controlled by wet removal, that dominates over dry deposition in the mid-Atlantic region (Ridley et al., 2012). It is unclear whether this bias is connected to a poor representation of the Saharan Air Layer (SAL) at present model resolution or an unidentified source of systematic bias. Higher resolution simulations will be required to capture the structure of the SAL, which can act as a conveyor for dust across the Atlantic. Excessive removal of dust will bias modeled dust lifetime low and result in a conservative observational dust AOD estimate because of the regional to global scaling employed in this study. The range of model dust lifetimes results in 13% to 23% of the global dust AOD coming from regions outside of those considered explicitly in this study. This constitutes a ±5% (0.0016) uncertainty in the observational global dust AOD estimate (Table 1); therefore, based on the comparison of dust AOD in the mid-Atlantic it is plausible that the actual global dust AOD is towards the upper limit of this uncertainty bound. While the model underestimation of mid-Atlantic dust may not be a major factor in the global dust AOD, it could have important implications for the simulation of hurricane genesis and nutrient deposition in the Amazon.

The models consistently underestimate AOD over Asian desert regions throughout most seasons. The low bias is present across all models and in all seasons except fall, when dust AOD is relatively low. The greatest divergence between models and observations occurs at the Taklamakan desert in spring and summer, when dust emissions are at their peak. However, there is some discrepancy between the MODIS and MISR dust AOD during winter and spring. Some of the increase in MODIS dust AOD is present south of the Taklamakan desert, on the raised Tibetan Plateau. Although dust can be transported out of the basin onto the Tibetan Plateau (Chen et al., 2013) the magnitude of the AOD reported by MODIS is unexpected; therefore, we expect the MISR dust AOD to better represent this region. There is also considerable spread between observations in the Gobi Desert; however, the models are all biased low, except for spring when GEOS-Chem and WRF-Chem capture the seasonal peak in dust AOD. Seasonality is well captured by most models in the Thar desert, located between India and Pakistan, despite the general lack of dust AOD relative to the MODIS retrieved dust observations (Figure 9).

In the Middle East, the model dust AOD is biased slightly low relative to observations. We find general agreement between the modeled and observed seasonality, with few systematic biases across all models. However, all but MERRAero overemphasize summer dust at the expense of winter in the Kyzyl Kum region. CESM produces too much dust in summer,

Atmos. Chem. Phys. Discuss., doi:10.5194/acp-2016-385, 2016
Manuscript under review for journal Atmos. Chem. Phys.
Published: 20 May 2016

relative to other seasons, driven by high dust AOD between the Southern Middle East and Kyzyl Kum regions (the Gulf of Oman) that is present, but weaker, in the satellite observations.

Considering the southern hemispheric regions, our analysis indicates that the simulated dust AOD is comparable in Australia and lower than observed in South Africa and South America. However, the uncertainty in the observational dust AOD is too large to draw quantitative conclusions about the model representation of dust in those regions.

Throughout the comparison we find that MERRAero generally provides better dust AOD seasonal agreement with the observational estimates than the other models. This is expected as the MERRAero simulation involves assimilation of MODIS AOD retrievals (Buchard et al., 2015) and is therefore not independent from the observations to which we are comparing. Furthermore, MERRAero is also produced at a higher resolution than the other models (0.625° x 0.5°) which may further contribute to better representation of dust emissions owing to more spatially resolved surface winds. However, the magnitude of the global dust AOD provided by the MERRAero simulation is the lowest of the four models (0.027) and is only just within the 2σ uncertainty bound on the observationally-constrained dust AOD estimate. The total global AOD for all species in MERRAero is 5% - 15% higher than the other models, while dust accounts for a smaller fraction of the AOD in MERRAero (20%) than the other models (24% - 26%). This can be interpreted in two ways: either the contribution of dust to the total AOD is conservative in MERRAero, or the observationally-constrained estimates are biased high owing to a persistent low bias of non-dust AOD in 3 of the 4 models. For this reason, we present the observational-estimate with a 2σ uncertainty to encompass the range of realistic global dust AOD estimates.

5 Conclusions

To provide an observational constraint for the global dust AOD we use three satellite retrievals of AOD over a 5-year period, use AERONET observations to correct biases in the satellite retrievals, and use speciated aerosol AOD from four global chemical transport models to separate the contributions of dust and non-dust AOD. Throughout the analysis we use bootstrapping to retain a robust estimate of the uncertainty on the dust AOD. We determine the global dust AOD to be 0.033 ± 0.006 (2σ), with all but 3 of the satellite-model combinations in this study yielding a larger dust AOD than the median of the 15 AeroCom models (0.029 ± 0.011). The observational estimate narrows the likely range of dust AOD greatly from that presented by the model estimates. The observational dust AOD is presented as seasonal averages for 5 years (2004-2008) across 15 regions, providing a dataset with which the broad performance of model dust schemes can be evaluated (available by request to the author).

Two of the four models used in this study are within the one standard deviation uncertainty of the observational estimate, the other two fall below the average. Using the regional and seasonal estimates of dust AOD, we highlight three general discrepancies between the models and observations: (1) the dust AOD across most of North Africa is overestimated in the models; (2) the Asian and some Middle-Eastern deserts are underrepresented, (3) modeled seasonality varies considerably between models but generally overestimates winter and spring dust at the expense of summer in Africa, and overestimate fall

dust at the expense of spring in Asian deserts, and (4) removal of dust exported across the Atlantic appears to be too strong in the models, which may indicate a systematic underestimation of dust lifetimes. We have used the observationally-constrained estimate of dust AOD to isolate specific regions in which the models disagree with the observations. However, the underlying mechanisms for the discrepancies are unclear and may be driven by the assumed physical characteristics of the surface, by the representation of surface wind, by the subsequent transport and deposition, or likely a combination of all factors. Further research in the areas highlighted in this work is expected to improve model simulations, and hence future estimates of the radiative, human health, and biosphere interactions of mineral dust.

Acknowledgements

This work was supported by NASA under grant NN14AP38G. J.F.K. acknowledges support from the National Science Foundation (NSF) under grant 1552519. Chun Zhao is supported by the U.S. Department of Energy (DOE) as part of the Regional & Global Climate Modeling (RGCM) program.

References

Albani, S., Mahowald, N. M., Perry, A. T., Scanza, R. A., Zender, C. S., Heavens, N. G., Maggi, V., Kok, J. F. and Otto-Bliesner, B. L.: Improved dust representation in the Community Atmosphere Model, J. Adv. Model. Earth Syst., n/a–n/a, doi:10.1002/2013MS000279, 2014.

Alexander, B., Park, R. J., Jacob, D. J., Li, Q. B., Yantosca, R. M., Savarino, J., Lee, C. C. W. and Thiemens, M. H.: Sulfate formation in sea-salt aerosols: Constraints from oxygen isotopes, J. Geophys. Res.-Atmospheres, 110(D10), doi:10.1029/2004JD005659, doi:D10307 Artn d10307, 2005.

Ångström, A.: The parameters of atmospheric turbidity, Tellus, 16(1), 64–75, doi:10.1111/j.2153-3490.1964.tb00144.x, 1964.

Balkanski, Y., Schulz, M., Claquin, T. and Guibert, S.: Reevaluation of Mineral aerosol radiative forcings suggests a better agreement with satellite and AERONET data, Atmospheric Chem. Phys., 7, 81–95, 2007.

Barnard, J. C., Fast, J. D., Paredes-Miranda, G., Arnott, W. P. and Laskin, A.: Technical Note: Evaluation of the WRF-Chem "Aerosol Chemical to Aerosol Optical Properties" Module using data from the MILAGRO campaign, Atmos Chem Phys, 10(15), 7325–7340, doi:10.5194/acp-10-7325-2010, 2010.

Boucher, O., Randall, D., Artaxo, P., Bretherton, C., Feingold, G., Forster, P., Kerminen, V.-M., Kondo, Y., Liao, H. and Lohmann, U.: Clouds and aerosols, in Climate change 2013: The physical science basis. Contribution of working group I to the fifth assessment report of the intergovernmental panel on climate change, pp. 571–657, Cambridge University Press., 2013.

Buchard, V., da Silva, A. M., Colarco, P., Krotkov, N., Dickerson, R. R., Stehr, J. W., Mount, G., Spinei, E., Arkinson, H. L. and He, H.: Evaluation of GEOS-5 sulfur dioxide simulations during the Frostburg, MD 2010 field campaign, Atmos Chem Phys, 14(4), 1929–1941, doi:10.5194/acp-14-1929-2014, 2014.

Buchard, V., Silva, A. M. da, Colarco, P. R., Darmenov, A., Randles, C. A., Govindaraju, R., Torres, O., Campbell, J. and Spurr, R.: Using the OMI aerosol index and absorption aerosol optical depth to evaluate the NASA MERRA Aerosol Reanalysis, Atmospheric Chem. Phys., 15(10), 5743, doi:http://dx.doi.org/10.5194/acp-15-5743-2015, 2015.

Buchard, V., da Silva, A. M., Randles, C. A., Colarco, P., Ferrare, R., Hair, J., Hostetler, C., Tackett, J. and Winker, D.: Evaluation of the surface PM2.5 in Version 1 of the NASA MERRA Aerosol Reanalysis over the United States, Atmos. Environ., 125, Part A, 100–111, doi:10.1016/j.atmosenv.2015.11.004, 2016.

Chen, S., Huang, J., Zhao, C., Qian, Y., Leung, L. R. and Yang, B.: Modeling the transport and radiative forcing of Taklimakan dust over the Tibetan Plateau: A case study in the summer of 2006, J. Geophys. Res. Atmospheres, 118(2), 797–812, doi:10.1002/jgrd.50122, 2013.

Chin, M., Ginoux, P., Kinne, S., Torres, O., Holben, B. N., Duncan, B. N., Martin, R. V., Logan, J. A., Higurashi, A. and Nakajima, T.: Tropospheric aerosol optical thickness from the GOCART model and comparisons with satellite and Sun photometer measurements, J. Atmospheric Sci., 59(3), 461–483, 2002.

Colarco, P., da Silva, A., Chin, M. and Diehl, T.: Online simulations of global aerosol distributions in the NASA GEOS-4 model and comparisons to satellite and ground-based aerosol optical depth, J. Geophys. Res. Atmospheres, 115(D14), D14207, doi:10.1029/2009JD012820, 2010.

Dee, D. P., Uppala, S. M., Simmons, A. J., Berrisford, P., Poli, P., Kobayashi, S., Andrae, U., Balmaseda, M. A., Balsamo, G., Bauer, P., Bechtold, P., Beljaars, A. C. M., van de Berg, L., Bidlot, J., Bormann, N., Delsol, C., Dragani, R., Fuentes, M., Geer, A. J., Haimberger, L., Healy, S. B., Hersbach, H., Hólm, E. V., Isaksen, L., Kållberg, P., Köhler, M., Matricardi, M., McNally, A. P., Monge-Sanz, B. M., Morcrette, J.-J., Park, B.-K., Peubey, C., de Rosnay, P., Tavolato, C., Thépaut, J.-N. and Vitart, F.: The ERA-Interim reanalysis: configuration and performance of the data assimilation system, Q. J. R. Meteorol. Soc., 137(656), 553–597, doi:10.1002/qj.828, 2011.

van Donkelaar, A., Martin, R. V. and Park, R. J.: Estimating ground-level PM2.5 using aerosol optical depth determined from satellite remote sensing, J. Geophys. Res.-Atmospheres, 111(D21), doi:D21201 Artn d21201, 2006.

Drury, E., Jacob, D. J., Spurr, R. J. ., Wang, J., Shinozuka, Y., Anderson, B. E., Clarke, A. D., Dibb, J., McNaughton, C. and Weber, R.: Synthesis of satellite (MODIS), aircraft (ICARTT), and surface (IMPROVE, EPA-AQS, AERONET) aerosol observations over eastern North America to improve MODIS aerosol retrievals and constrain surface aerosol concentrations and sources, J. Geophys. Res., 115(D14), D14204, 2010.

Eck, T. F., Holben, B. N., Reid, J. S., Dubovik, O., Smirnov, A., O'Neill, N. T., Slutsker, I. and Kinne, S.: Wavelength dependence of the optical depth of biomass burning, urban, and desert dust aerosols, J. Geophys. Res. Atmospheres, 104(D24), 31333–31349, doi:10.1029/1999JD900923, 1999.

Eck, T. F., Holben, B. N., Reid, J. S., Arola, A., Ferrare, R. A., Hostetler, C. A., Crumeyrolle, S. N., Berkoff, T. A., Welton, E. J., Lolli, S., Lyapustin, A., Wang, Y., Schafer, J. S., Giles, D. M., Anderson, B. E., Thornhill, K. L., Minnis, P., Pickering, K. E., Loughner, C. P., Smirnov, A. and Sinyuk, A.: Observations of rapid aerosol optical depth enhancements in the vicinity of polluted cumulus clouds, Atmos Chem Phys, 14(21), 11633–11656, doi:10.5194/acp-14-11633-2014, 2014.

Efron, B. and Gong, G.: A Leisurely Look at the Bootstrap, the Jackknife, and Cross-Validation, Am. Stat., 37(1), 36–48, doi:10.1080/00031305.1983.10483087, 1983.

Evan, A. T., Flamant, C., Fiedler, S. and Doherty, O.: An analysis of aeolian dust in climate models, Geophys. Res. Lett., 41(16), 2014GL060545, doi:10.1002/2014GL060545, 2014.

Evans, J., van Donkelaar, A., Martin, R. V., Burnett, R., Rainham, D. G., Birkett, N. J. and Krewski, D.: Estimates of global mortality attributable to particulate air pollution using satellite imagery, Environ. Res., 120, 33–42, doi:10.1016/j.envres.2012.08.005, 2013.

Fairlie, T. D., Jacob, D. J. and Park, R. J.: The impact of transpacific transport of mineral dust in the United States, Atmos. Environ., 41(6), 1251–1266, 2007.

Fast, J. D., Gustafson, W. I., Easter, R. C., Zaveri, R. A., Barnard, J. C., Chapman, E. G., Grell, G. A. and Peckham, S. E.: Evolution of ozone, particulates, and aerosol direct radiative forcing in the vicinity of Houston using a fully coupled meteorology-chemistry-aerosol model, J. Geophys. Res. Atmospheres, 111(D21), D21305, doi:10.1029/2005JD006721, 2006.

Ford, B. and Heald, C. L.: Exploring the uncertainty associated with satellite-based estimates of premature mortality due to exposure to fine particulate matter, Atmospheric Chem. Phys. Discuss., 15(18), 25329–25380, doi:10.5194/acpd-15-25329-2015, 2015.

Fountoukis, C. and Nenes, A.: ISORROPIA II: a computationally efficient thermodynamic equilibrium model for K+-Ca2+-Mg2+-Nh(4)(+)-Na+-SO42--NO3--Cl--H2O aerosols, Atmos Chem Phys, 7(17), 4639–4659, 2007.

French, N. H. F., Goovaerts, P. and Kasischke, E. S.: Uncertainty in estimating carbon emissions from boreal forest fires, J. Geophys. Res. Atmospheres, 109(D14), D14S08, doi:10.1029/2003JD003635, 2004.

Ginoux, P., Chin, M., Tegen, I., Prospero, J. M., Holben, B., Dubovik, O. and Lin, S.-J.: Sources and distributions of dust aerosols simulated using the GOCART model, J Geophys Res, 106(D17), 20255–20273, 2001.

Ginoux, P., Prospero, J. M., Gill, T. E., Hsu, N. C. and Zhao, M.: Global-scale attribution of anthropogenic and natural dust sources and their emission rates based on MODIS Deep Blue aerosol products, Rev. Geophys., 50(3), doi:10.1029/2012RG000388, 2012.

Gong, S.: A parameterization of sea-salt aerosol source function for sub- and super-micron particles, Glob. Biochem Cycles, 17(4), 1097, 2003.

Heald, C. L. and Spracklen, D. V.: Land Use Change Impacts on Air Quality and Climate, Chem. Rev., 115(10), 4476–4496, doi:10.1021/cr500446g, 2015.

Heald, C. L., Ridley, D. A., Kroll, J. H., Barrett, S. R. H., Cady-Pereira, K. E., Alvarado, M. J. and Holmes, C. D.: Contrasting the direct radiative effect and direct radiative forcing of aerosols, Atmos Chem Phys, 14(11), 5513–5527, doi:10.5194/acp-14-5513-2014, 2014.

Hess, M., Koepke, P. and Schult, I.: Optical propeties of aerosol and clouds: The software package OPAC, Bull Am Meteorol Soc, 79, 831–844, 1998a.

Hess, M., Koepke, P. and Schult, I.: Optical propeties of aerosol and clouds: The software package OPAC, Bull Am Meteorol Soc, 79, 831–844, 1998b.

Holben, B. N., Eck, T. F., Slutsker, I., Tanré, D., Buis, J. P., Setzer, A., Vermote, E., Reagan, J. A., Kaufman, Y. J., Nakajima, T., Lavenu, F., Jankowiak, I. and Smirnov, A.: AERONET—A Federated Instrument Network and Data Archive for Aerosol Characterization, Remote Sens. Environ., 66(1), 1–16, doi:10.1016/S0034-4257(98)00031-5, 1998.

Hsu, N. C., Tsay, S. C., King, M. D. and Herman, J. R.: Deep blue retrievals of Asian aerosol properties during ACE-Asia, IEEE Trans Geosci Remote Sens., 44(11), 3180–3195, doi:10.1109/tgrs.2006.879540, 2006.

Huneeus, N., Schulz, M., Balkanski, Y., Griesfeller, J., Prospero, J., Kinne, S., Bauer, S., Boucher, O., Chin, M., Dentener, F., Diehl, T., Easter, R., Fillmore, D., Ghan, S., Ginoux, P., Grini, A., Horowitz, L., Koch, D., Krol, M. C., Landing, W., Liu, X., Mahowald, N., Miller, R., Morcrette, J.-J., Myhre, G., Penner, J., Perlwitz, J., Stier, P., Takemura, T. and Zender, C. S.: Global dust model intercomparison in AeroCom phase I, Atmos Chem Phys, 11(15), 7781–7816, doi:10.5194/acp-11-7781-2011, 2011.

Hurrell, J. W.: 2011 Community Earth System Model (cesm) Tutorial, August 1-5, 2011, University Corporation for Atmospheric Research. [online] Available from: http://www.osti.gov/scitech/biblio/1096191 (Accessed 7 April 2016), 2013.

Hu, Z., Zhao, C., Huang, J., Leung, L. R., Qian, Y., Yu, H., Huang, L. and Kalashnikova, O. V.: Trans-pacific transport and evolution of aerosols: Evaluation of quasi global WRF-Chem simulation with multiple observations, Geosci. Model Dev. Discuss., 1–65, doi:10.5194/gmd-2015-248, 2016.

Jaeglé, L., Quinn, P. K., Bates, T. S., Alexander, B. and Lin, J.-T.: Global distribution of sea salt aerosols: new constraints from in situ and remote sensing observations, Atmospheric Chem. Phys., 11(7), 3137–3157, doi:10.5194/acp-11-3137-2011, 2011.

Jin, Q., Wei, J., Yang, Z.-L., Pu, B. and Huang, J.: Consistent response of Indian summer monsoon to Middle East dust in observations and simulations, Atmos Chem Phys, 15(17), 9897–9915, doi:10.5194/acp-15-9897-2015, 2015.

Kahn, R. A., Gaitley, B. J., Garay, M. J., Diner, D. J., Eck, T. F., Smirnov, A. and Holben, B. N.: Multiangle Imaging SpectroRadiometer global aerosol product assessment by comparison with the Aerosol Robotic Network, J Geophys Res-Atmos, 115, 28, doi:D23209 10.1029/2010jd014601, 2010.

Kok, J. F.: A scaling theory for the size distribution of emitted dust aerosols suggests climate models underestimate the size of the global dust cycle, Proc. Natl. Acad. Sci., 108(3), 1016–1021, 2011a.

Kok, J. F.: Does the size distribution of mineral dust aerosols depend on the wind speed at emission?, Atmos Chem Phys, 11(19), 10149–10156, doi:10.5194/acp-11-10149-2011, 2011b.

Kok, J. F., Mahowald, N. M., Fratini, G., Gillies, J. A., Ishizuka, M., Leys, J. F., Mikami, M., Park, M.-S., Park, S.-U., Van Pelt, R. S. and Zobeck, T. M.: An improved dust emission model – Part 1: Model description and comparison against measurements, Atmos Chem Phys, 14(23), 13023–13041, doi:10.5194/acp-14-13023-2014, 2014a.

Kok, J. F., Albani, S., Mahowald, N. M. and Ward, D. S.: An improved dust emission model – Part 2: Evaluation in the Community Earth System Model, with implications for the use of dust source functions, Atmos Chem Phys, 14(23), 13043–13061, doi:10.5194/acp-14-13043-2014, 2014b.

Koren, I., Remer, L. A., Kaufman, Y. J., Rudich, Y. and Martins, J. V.: On the twilight zone between clouds and aerosols, Geophys. Res. Lett., 34(8), L08805, doi:10.1029/2007GL029253, 2007.

Lamarque, J.-F., Emmons, L. K., Hess, P. G., Kinnison, D. E., Tilmes, S., Vitt, F., Heald, C. L., Holland, E. A., Lauritzen, P. H., Neu, J., Orlando, J. J., Rasch, P. J. and Tyndall, G. K.: CAM-chem: description and evaluation of interactive atmospheric chemistry in the Community Earth System Model, Geosci Model Dev, 5(2), 369–411, doi:10.5194/gmd-5-369-2012, 2012.

Leibensperger, E. M., Mickley, L. J., Jacob, D. J., Chen, W.-T., Seinfeld, J. H., Nenes, A., Adams, P. J., Streets, D. G., Kumar, N. and Rind, D.: Climatic effects of 1950–2050 changes in US anthropogenic aerosols – Part 1: Aerosol trends and radiative forcing, Atmos Chem Phys, 12(7), 3333–3348, doi:10.5194/acp-12-3333-2012, 2012.

Levy, R. C., Remer, L. A., Kleidman, R. G., Mattoo, S., Ichoku, C., Kahn, R. and Eck, T. F.: Global evaluation of the Collection 5 MODIS dark-target aerosol products over land, Atmos Chem Phys, 10(21), 10399–10420, doi:10.5194/acp-10-10399-2010, 2010.

Levy, R. C., Mattoo, S., Munchak, L. A., Remer, L. A., Sayer, A. M., Patadia, F. and Hsu, N. C.: The Collection 6 MODIS aerosol products over land and ocean, Atmos Meas Tech, 6(11), 2989–3034, doi:10.5194/amt-6-2989-2013, 2013.

Lim, S. S., Vos, T., Flaxman, A. D., Danaei, G., Shibuya, K., Adair-Rohani, H., AlMazroa, M. A., Amann, M., Anderson, H. R., Andrews, K. G., Aryee, M., Atkinson, C., Bacchus, L. J., Bahalim, A. N., Balakrishnan, K., Balmes, J., Barker-Collo, S., Baxter, A., Bell, M. L., Blore, J. D., Blyth, F., Bonner, C., Borges, G., Bourne, R., Boussinesq, M., Brauer, M., Brooks, P., Bruce, N. G., Brunekreef, B., Bryan-Hancock, C., Bucello, C., Buchbinder, R., Bull, F., Burnett, R. T., Byers, T. E., Calabria, B., Carapetis, J., Carnahan, E., Chafe, Z., Charlson, F., Chen, H., Chen, J. S., Cheng, A. T.-A., Child, J. C., Cohen, A., Colson, K. E., Cowie, B. C., Darby, S., Darling, S., Davis, A., Degenhardt, L., Dentener, F., Des Jarlais, D. C., Devries, K., Dherani, M., Ding, E. L., Dorsey, E. R., Driscoll, T., Edmond, K., Ali, S. E., Engell, R. E., Erwin, P. J., Fahimi, S., Falder, G., Farzadfar, F., Ferrari, A., Finucane, M. M., Flaxman, S., Fowkes, F. G. R., Freedman, G., Freeman, M. K., Gakidou, E., Ghosh, S., Giovannucci, E., Gmel, G., Graham, K., Grainger, R., Grant, B., Gunnell, D., Gutierrez, H. R., Hall, W., Hoek, H. W., Hogan, A., Hosgood III, H. D., Hoy, D., Hu, H., Hubbell, B. J., Hutchings, S. J., Ibeanusi, S. E., Jacklyn, G. L., Jasrasaria, R., Jonas, J. B., Kan, H., Kanis, J. A., Kassebaum, N., Kawakami, N., Khang, Y.-H., Khatibzadeh, S., Khoo, J.-P., et al.: A comparative risk assessment of burden of disease and injury attributable to 67 risk factors and risk factor clusters in 21 regions, 1990–2010: a systematic analysis for the Global Burden of Disease Study 2010, The Lancet, 380(9859), 2224–2260, doi:10.1016/S0140-6736(12)61766-8, 2012.

Liu, X., Easter, R. C., Ghan, S. J., Zaveri, R., Rasch, P., Shi, X., Lamarque, J.-F., Gettelman, A., Morrison, H., Vitt, F., Conley, A., Park, S., Neale, R., Hannay, C., Ekman, A. M. L., Hess, P., Mahowald, N., Collins, W., Iacono, M. J., Bretherton, C. S., Flanner, M. G. and Mitchell, D.: Toward a minimal representation of aerosols in climate models: description and evaluation in the Community Atmosphere Model CAM5, Geosci Model Dev, 5(3), 709–739, doi:10.5194/gmd-5-709-2012, 2012.

Lu, Z., Zhang, Q. and Streets, D. G.: Sulfur dioxide and primary carbonaceous aerosol emissions in China and India, 1996–2010, Atmos Chem Phys, 11(18), 9839–9864, doi:10.5194/acp-11-9839-2011, 2011.

Mahowald, N. M., Muhs, D. R., Levis, S., Rasch, P. J., Yoshioka, M., Zender, C. S. and Luo, C.: Change in atmospheric mineral aerosols in response to climate: Last glacial period, preindustrial, modern, and doubled carbon dioxide climates, J. Geophys. Res. Atmospheres, 111(D10), D10202, doi:10.1029/2005JD006653, 2006.

Mahowald, N. M., Kloster, S., Engelstaedter, S., Moore, J. K., Mukhopadhyay, S., McConnell, J. R., Albani, S., Doney, S. C., Bhattacharya, A., Curran, M. A. J., Flanner, M. G., Hoffman, F. M., Lawrence, D. M., Lindsay, K., Mayewski, P. A., Neff, J., Rothenberg, D., Thomas, E., Thornton, P. E. and Zender, C. S.: Observed 20th century desert dust variability: impact on climate and biogeochemistry, Atmospheric Chem. Phys., 10(22), 10875–10893, doi:10.5194/acp-10-10875-2010, 2010.

Mann, G. W., Carslaw, K. S., Reddington, C. L., Pringle, K. J., Schulz, M., Asmi, A., Spracklen, D. V., Ridley, D. A., Woodhouse, M. T., Lee, L. A., Zhang, K., Ghan, S. J., Easter, R. C., Liu, X., Stier, P., Lee, Y. H., Adams, P. J., Tost, H., Lelieveld, J., Bauer, S. E., Tsigaridis, K., van Noije, T. P. C., Strunk, A., Vignati, E., Bellouin, N., Dalvi, M., Johnson, C. E., Bergman, T., Kokkola, H., von Salzen, K., Yu, F., Luo, G., Petzold, A., Heintzenberg, J., Clarke, A., Ogren, J. A., Gras, J., Baltensperger, U., Kaminski, U., Jennings, S. G., O'Dowd, C. D., Harrison, R. M., Beddows, D. C. S., Kulmala, M., Viisanen, Y., Ulevicius, V., Mihalopoulos, N., Zdimal, V., Fiebig, M., Hansson, H.-C., Swietlicki, E. and Henzing, J. S.: Intercomparison and evaluation of global aerosol microphysical properties among AeroCom models of a range of complexity, Atmos Chem Phys, 14(9), 4679–4713, doi:10.5194/acp-14-4679-2014, 2014.

Marshak, A., Wen, G., Coakley, J. A., Remer, L. A., Loeb, N. G. and Cahalan, R. F.: A simple model for the cloud adjacency effect and the apparent bluing of aerosols near clouds, J. Geophys. Res. Atmospheres, 113(D14), D14S17, doi:10.1029/2007JD009196, 2008.

Martin, R. V., Jacob, D. J., Yantosca, R. M., Chin, M. and Ginoux, P.: Global and regional decreases in tropospheric oxidants from photochemical effects of aerosols, J. Geophys. Res.-Atmospheres, 108(D3), doi:10.1029/2002JD002622, 2003.

Martonchik, J. V., Diner, D. J., Kahn, R. A., Ackerman, T. P., Verstraete, M. E., Pinty, B. and Gordon, H. R.: Techniques for the retrieval of aerosol properties over land and ocean using multiangle imaging, IEEE Trans Geosci Remote Sens., 36(4), 1212–1227, 1998.

Martonchik, J. V., Diner, D. J., Kahn, R., Gaitley, B. and Holben, B. N.: Comparison of MISR and AERONET aerosol optical depths over desert sites, Geophys Res Lett, 31(16), 4, doi:L16102 10.1029/2004gl019807, 2004.

Matichuk, R. I., Colarco, P. R., Smith, J. A. and Toon, O. B.: Modeling the transport and optical properties of smoke aerosols from African savanna fires during the Southern African Regional Science Initiative campaign (SAFARI 2000), J. Geophys. Res.-Atmospheres, 112(D8), doi:10.1029/2006JD007528, doi:D08203 Artn d08203, 2007.

Mishra, S. K., Dey, S. and Tripathi, S. N.: Implications of particle composition and shape to dust radiative effect: A case study from the Great Indian Desert, Geophys. Res. Lett., 35(23), L23814, doi:10.1029/2008GL036058, 2008.

Moon, T., Wang, Y., Liu, Y. and Yu, B.: Evaluation of a MISR-Based High-Resolution Aerosol Retrieval Method Using AERONET DRAGON Campaign Data, IEEE Trans. Geosci. Remote Sens., 53(8), 4328–4339, doi:10.1109/TGRS.2015.2395722, 2015.

Muller, D., Mattis, I., Wandinger, U., Ansmann, A., Althausen, D., Dubovik, O., Eckhardt, S. and Stohl, A.: Saharan dust over a central European EARLINET-AERONET site: Combined observations with Raman lidar and Sun photometer, J. Geophys. Res.-Atmospheres, 108(D12), 2003.

Neale, R. B., Chen, C.-C., Gettelman, A., Lauritzen, P. H., Park, S., Williamson, D. L., Conley, A. J., Garcia, R., Kinnison, D., Lamarque, J.-F. and others: Description of the NCAR community atmosphere model (CAM 5.0), NCAR Tech Note NCARTN-486 STR [online] Available from: https://www.ccsm.ucar.edu/models/ccsm4.0/cam/docs/description/cam4_desc.pdf (Accessed 8 April 2016), 2010.

Olivier, J. G. J.: Applications of EDGAR Including a description of EDGAR 3.0: reference database with trend data for 1970-1995, Natl. Inst. of Public Health and Environ., Bilthoven, Netherlands., 2001.

O'Neill, N. T., Dubovik, O. and Eck, T. F.: Modified Ångström exponent for the characterization of submicrometer aerosols, Appl. Opt., 40(15), 2368, doi:10.1364/AO.40.002368, 2001.

Pantillon, F., Knippertz, P., Marsham, J. H., Panitz, H.-J. and Bischoff-Gauss, I.: Modeling haboob dust storms in large-scale weather and climate models, J. Geophys. Res. Atmospheres, 2015JD024349, doi:10.1002/2015JD024349, 2016.

Park, R. J., Jacob, D. J., Chin, M. and Martin, R. V.: Sources of carbonaceous aerosols over the United States and implications for natural visibility, J. Geophys. Res.-Atmospheres, 108(D12), doi:10.1029/2002JD003190, doi:4355 Artn 4355, 2003.

Park, R. J., Jacob, D. J., Field, B. D., Yantosca, R. M. and Chin, M.: Natural and transboundary pollution influences on sulfate-nitrate-ammonium aerosols in the United States: Implications for policy, J. Geophys. Res.-Atmospheres, 109(D15), doi:10.1029/2003JD004473, 2004.

Park, R. J., Jacob, D. J., Kumar, N. and Yantosca, R. M.: Regional visibility statistics in the United States: Natural and transboundary pollution influences, and implications for the Regional Haze Rule, Atmos. Environ., 40(28), 5405–5423, 2006.

Prasad, A. K. and Singh, R. P.: Changes in aerosol parameters during major dust storm events (2001-2005) over the Indo-Gangetic Plains using AERONET and MODIS data, J. Geophys. Res.-Atmospheres, 112(D9), 2007.

Prospero, J. M.: African dust: Its large-scale transport over the Atlantic ocean and its impact on the Mediterranean region, in Regional Climate Variability and Its Impacts in the Mediterranean Area, pp. 15–38., 2007.

Prospero, J. M., Ginoux, P., Torres, O., Nicholson, S. E. and Gill, T. E.: Environmental characterization of global sources of atmospheric soil dust identified with the Nimbus 7 Total Ozone Mapping Spectrometer (TOMS) absorbing aerosol product, Rev Geophys, 40(1), 31, doi:1002 10.1029/2000rg000095, 2002.

Prospero, J. M., Collard, F.-X., Molinié, J. and Jeannot, A.: Characterizing the annual cycle of African dust transport to the Caribbean Basin and South America and its impact on the environment and air quality, Glob. Biogeochem. Cycles, 28(7), 2013GB004802, doi:10.1002/2013GB004802, 2014.

Pye, H. O. T. and Seinfeld, J. H.: A global perspective on aerosol from low-volatility organic compounds, Atmospheric Chem. Phys., 10, 4377–4401, doi:10.5194/acp-10-4377-2010, 2010.

Pye, H. O. T., Chan, A. W. H., Barkley, M. P. and Seinfeld, J. H.: Global modeling of organic aerosol: the importance of reactive nitrogen (NOx and NO3), Atmos Chem Phys, 10(22), 11261–11276, doi:10.5194/acp-10-11261-2010, 2010.

Quaas, J., Stevens, B., Stier, P. and Lohmann, U.: Interpreting the cloud cover – aerosol optical depth relationship found in satellite data using a general circulation model, Atmos Chem Phys, 10(13), 6129–6135, doi:10.5194/acp-10-6129-2010, 2010.

Rasch, P. J., Collins, W. D. and Eaton, B. E.: Understanding the Indian Ocean Experiment (INDOEX) aerosol distributions with an aerosol assimilation, J. Geophys. Res.-Atmospheres, 106(D7), 7337–7355, 2001.

Reddington, C. L., Spracklen, D. V., Artaxo, P., Ridley, D., Rizzo, L. V. and Arana, A.: Analysis of particulate emissions from tropical biomass burning using a global aerosol model and long-term surface observations, Atmospheric Chem. Phys. Discuss., 1–49, doi:10.5194/acp-2015-967, 2016.

Reid, J. S., Eck, T. F., Christopher, S. A., Hobbs, P. V. and Holben, B.: Use of the Ångstrom exponent to estimate the variability of optical and physical properties of aging smoke particles in Brazil, J. Geophys. Res. Atmospheres, 104(D22), 27473–27489, doi:10.1029/1999JD900833, 1999.

Remer, L. A., Kaufman, Y. J., Tanré, D., Mattoo, S., Chu, D. A., Martins, J. V., Li, R.-R., Ichoku, C., Levy, R. C., Kleidman, R. G., Eck, T. F., Vermote, E. and Holben, B. N.: The MODIS Aerosol Algorithm, Products, and Validation, J. Atmospheric Sci., 62(4), 947–973, doi:10.1175/JAS3385.1, 2005.

Remer, L. A., Mattoo, S., Levy, R. C., Heidinger, A., Pierce, R. B. and Chin, M.: Retrieving aerosol in a cloudy environment: aerosol product availability as a function of spatial resolution, Atmos Meas Tech, 5(7), 1823–1840, doi:10.5194/amt-5-1823-2012, 2012.

Ridley, D. A., Heald, C. L. and Ford, B.: North African dust export and deposition: A satellite and model perspective, J. Geophys. Res., 117(D2), doi:10.1029/2011JD016794, 2012.

Ridley, D. A., Heald, C. L., Pierce, J. R. and Evans, M. J.: Toward resolution-independent dust emissions in global models: Impacts on the seasonal and spatial distribution of dust, Geophys. Res. Lett., 40(11), 2873–2877, doi:10.1002/grl.50409, 2013.

Ridley, D. A., Heald, C. L. and Prospero, J. M.: What controls the recent changes in African mineral dust aerosol across the Atlantic?, Atmos Chem Phys, 14(11), 5735–5747, doi:10.5194/acp-14-5735-2014, 2014.

Rienecker, M. M., Suarez, M. J., Gelaro, R., Todling, R., Bacmeister, J., Liu, E., Bosilovich, M. G., Schubert, S. D., Takacs, L., Kim, G.-K., Bloom, S., Chen, J., Collins, D., Conaty, A., da Silva, A., Gu, W., Joiner, J., Koster, R. D., Lucchesi, R., Molod, A., Owens, T., Pawson, S., Pegion, P., Redder, C. R., Reichle, R., Robertson, F. R., Ruddick, A. G., Sienkiewicz, M. and Woollen, J.: MERRA: NASA's Modern-Era Retrospective Analysis for Research and Applications, J. Clim., 24(14), 3624–3648, doi:10.1175/JCLI-D-11-00015.1, 2011.

Sayer, A. M., Hsu, N. C., Bettenhausen, C. and Jeong, M.-J.: Validation and uncertainty estimates for MODIS Collection 6 "Deep Blue" aerosol data, J. Geophys. Res. Atmospheres, 118(14), 7864–7872, doi:10.1002/jgrd.50600, 2013.

Silverman, B.: Density Estimation for Statistics and Data Analysis, Chapman and Hall., 1986.

Sinyuk, A., Torres, O. and Dubovik, O.: Combined use of satellite and surface observations to infer the imaginary part of refractive index of Saharan dust, Geophys. Res. Lett., 30(2), 2003.

Smirnov, A., Holben, B. N., Eck, T. F., Dubovik, O. and Slutsker, I.: Cloud-Screening and Quality Control Algorithms for the AERONET Database, Remote Sens. Environ., 73(3), 337–349, doi:10.1016/S0034-4257(00)00109-7, 2000.

Smirnov, A., Holben, B. N., Eck, T. F., Slutsker, I., Chatenet, B. and Pinker, R. T.: Diurnal variability of aerosol optical depth observed at AERONET (Aerosol Robotic Network) sites, Geophys. Res. Lett., 29(23), 2002.

Stauffer, D. R. and Seaman, N. L.: Use of Four-Dimensional Data Assimilation in a Limited-Area Mesoscale Model. Part I: Experiments with Synoptic-Scale Data, Mon. Weather Rev., 118(6), 1250–1277, doi:10.1175/1520-0493(1990)118<1250:UOFDDA>2.0.CO;2, 1990.

Streets, D. G., Bond, T. C., Carmichael, G. R., Fernandes, S. D., Fu, Q., He, D., Klimont, Z., Nelson, S. M., Tsai, N. Y., Wang, M. Q., Woo, J.-H. and Yarber, K. F.: An inventory of gaseous and primary aerosol emissions in Asia in the year 2000, J. Geophys. Res. Atmospheres, 108(D21), 8809, doi:10.1029/2002JD003093, 2003.

Streets, D. G., Zhang, Q., Wang, L. T., He, K. B., Hao, J. M., Wu, Y., Tang, Y. H. and Carmichael, G. R.: Revisiting China's CO emissions after the Transport and Chemical Evolution over the Pacific (TRACE-P) mission: Synthesis of inventories, atmospheric modeling, and observations, J. Geophys. Res.-Atmospheres, 111(D14), doi:10.1029/2006JD007118, doi:D14306 Artn d14306, 2006.

van der Werf, G. R., Randerson, J. T., Giglio, L., Collatz, G. J., Kasibhatla, P. S. and Arellano Jr., A. F.: Interannual variability in global biomass burning emissions from 1997 to 2004, Atmos Chem Phys, 6(11), 3423–3441, doi:10.5194/acp-6-3423-2006, 2006.

van der Werf, G. R., Randerson, J. T., Giglio, L., Collatz, G. J., Mu, M., Kasibhatla, P. S., Morton, D. C., DeFries, R. S., Jin, Y. and van Leeuwen, T. T.: Global fire emissions and the contribution of deforestation, savanna, forest, agricultural, and peat fires (1997–2009), Atmos Chem Phys, 10(23), 11707–11735, doi:10.5194/acp-10-11707-2010, 2010.

Yu, Y., Notaro, M., Liu, Z., Wang, F., Alkolibi, F., Fadda, E. and Bakhrjy, F.: Climatic controls on the interannual to decadal variability in Saudi Arabian dust activity: Toward the development of a seasonal dust prediction model, J. Geophys. Res. Atmospheres, 120(5), 2014JD022611, doi:10.1002/2014JD022611, 2015.

Zaveri, R. A. and Peters, L. K.: A new lumped structure photochemical mechanism for large-scale applications, J. Geophys. Res. Atmospheres, 104(D23), 30387–30415, doi:10.1029/1999JD900876, 1999.

Zaveri, R. A., Easter, R. C., Fast, J. D. and Peters, L. K.: Model for Simulating Aerosol Interactions and Chemistry (MOSAIC), J. Geophys. Res. Atmospheres, 113(D13), D13204, doi:10.1029/2007JD008782, 2008.

Zender, C. S.: Mineral Dust Entrainment and Deposition (DEAD) model: Description and 1990s dust climatology, J. Geophys. Res., 108(D14), doi:10.1029/2002JD002775, 2003.

Zhang, L., Kok, J. F., Henze, D. K., Li, Q. and Zhao, C.: Improving simulations of fine dust surface concentrations over the western United States by optimizing the particle size distribution, Geophys. Res. Lett., n/a–n/a, doi:10.1002/grl.50591, 2013.

Zhang, Q., Streets, D. G., Carmichael, G. R., He, K. B., Huo, H., Kannari, A., Klimont, Z., Park, I. S., Reddy, S., Fu, J. S., Chen, D., Duan, L., Lei, Y., Wang, L. T. and Yao, Z. L.: Asian emissions in 2006 for the NASA INTEX-B mission, Atmos Chem Phys, 9(14), 5131–5153, doi:10.5194/acp-9-5131-2009, 2009.

Zhao, C., Liu, X., Leung, L. R., Johnson, B., McFarlane, S. A., Gustafson Jr., W. I., Fast, J. D. and Easter, R.: The spatial distribution of mineral dust and its shortwave radiative forcing over North Africa: modeling sensitivities to dust emissions and aerosol size treatments, Atmos Chem Phys, 10(18), 8821–8838, doi:10.5194/acp-10-8821-2010, 2010.

Zhao, C., Ruby Leung, L., Easter, R., Hand, J. and Avise, J.: Characterization of speciated aerosol direct radiative forcing over California, J. Geophys. Res. Atmospheres, 118(5), 2372–2388, doi:10.1029/2012JD018364, 2013.

Zhao, C. Z. C., Liu, X., Leung, L. R. and Hagos, S.: Radiative impact of mineral dust on monsoon precipitation variability over West Africa, Atmospheric Chem. Phys., 11(5), 1879–1893, 2011.

Atmos. Chem. Phys. Discuss., doi:10.5194/acp-2016-385, 2016
Manuscript under review for journal Atmos. Chem. Phys.
Published: 20 May 2016

Atmospheric Chemistry and Physics Discussions

Tables

Source of uncertainty	Relative bias in global dust AOD	Relative contribution to uncertainty
Satellite retrieval of seasonal AOD	1%	+41%
Model non-dust AOD	±5%	+19%
Model regional-to-global scaling	±5%	+19%
AERONET bias correction (MODIS Aqua, MODIS Terra, MISR)	<1% (+6%, +1% -8%)	-12%** (3%, 2%, <1%)
Satellite retrieval spatial sampling *(MODIS Aqua, MODIS Terra, MISR)*	<1% (<1%, <1%, +1.3%)	-- (+7%, +7%, +50%)
Satellite retrieval diurnal sampling *(MODIS Aqua, MODIS Terra, MISR)*	-4% (-5%, -1%, -2%)	+2% (-1%, +2%, +3%)
Cloud filtering (>80%)	-13%	<1%
Inclusion of S.H. desert regions	<1%	+8%
Inclusion of Gulf of Guinea	+7%	+16%

Table 1 – Each source of uncertainty is assessed in terms of the impact upon the global dust AOD standard deviation and any bias. The sign of the relative uncertainty indicates whether the uncertainty yields a bias or is symmetrical about the average. For the model non-dust AOD and regional-to-global scaling the bias is defined as the difference between the upper and lower estimate of the global dust AOD when the source of uncertainty is isolated. Italicized uncertainties are explored but not incorporated into the global dust AOD uncertainty estimate. Values here are for correlated errors between neighboring 2 x 2.5 degree grid cells; assuming errors within a region are uncorrelated (i.e. a different number of sigma from the mean for each grid cell in an iteration) yields ~8x smaller uncertainty.

**** Acts to reduce the uncertainty by this amount, bringing satellite retrieval estimates closer together.**

Atmos. Chem. Phys. Discuss., doi:10.5194/acp-2016-385, 2016
Manuscript under review for journal Atmos. Chem. Phys.
Published: 20 May 2016

Atmospheric Chemistry and Physics Discussions

Figures

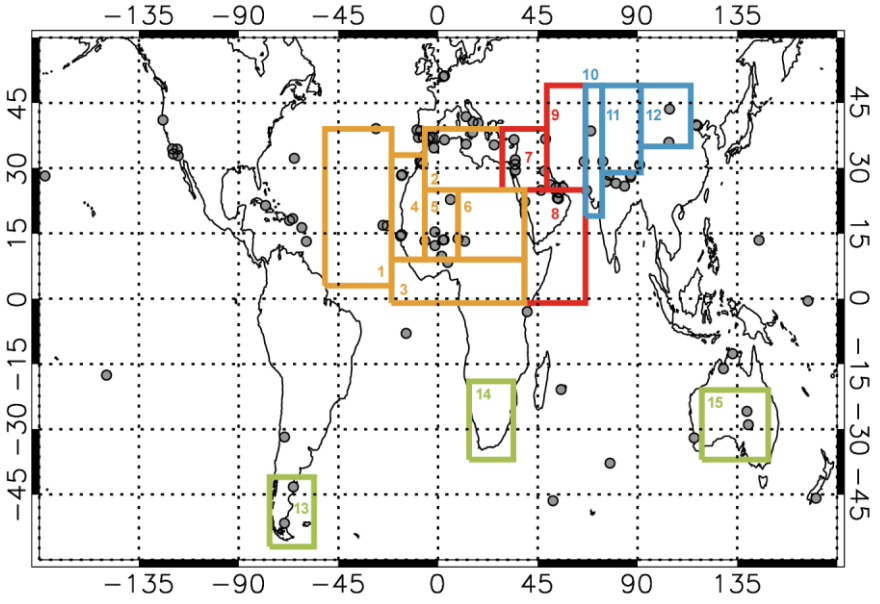

Figure 1 – The 15 regions considered explicitly in this study are defined. Regions are grouped into African (orange), Middle Eastern (red), Asian (blue), and Southern Hemispheric (green). AERONET sites used to bias correct satellite AOD are indicated with (gray circles). The regions are identified as (1) Mid-Atlantic, (2) N. Africa, (3) Gulf of Guinea, (4) W. Coast, (5) Atlas Mountains, (6) Bodele Depression, (7) N. Mid-East, (8) S. Mid-East, (9) Kyzyl Kum, (10) Thar, (11) Taklamakan, (12) Gobi, (13) S. America, (14) S. Africa, and (15) Australia.

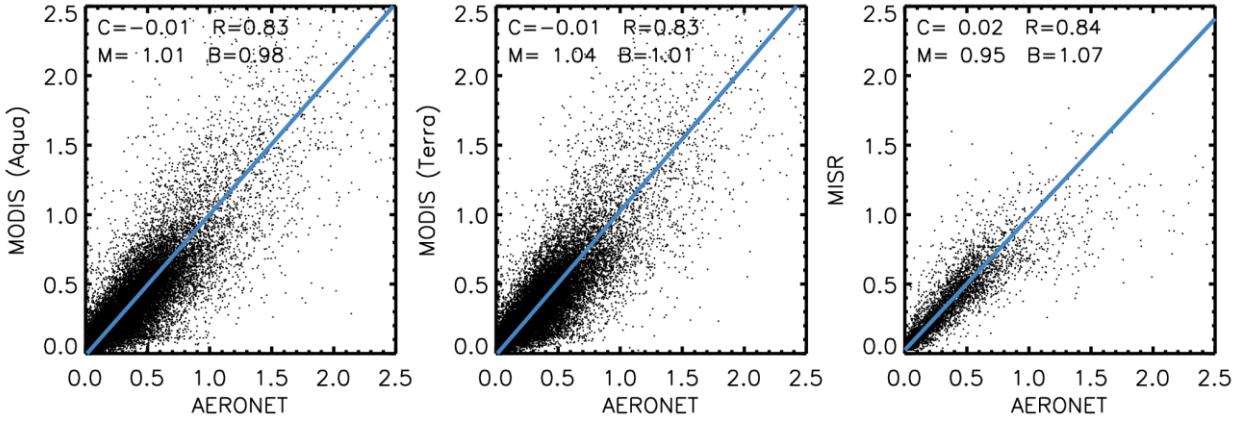

Figure 2 – Comparison of daily AOD from collocated AERONET and satellite retrievals. Only days when AERONET angstrom exponent is < 0.4 are used to focus on dust-influenced measurements. The linear regression is shown for each, along with the slope (M), intercept (C), correlation coefficient (R) and bias (B). For MISR, two regressions are performed, one for AOD<0.5 and one for AOD>0.5.

Atmos. Chem. Phys. Discuss., doi:10.5194/acp-2016-385, 2016
Manuscript under review for journal Atmos. Chem. Phys.
Published: 20 May 2016

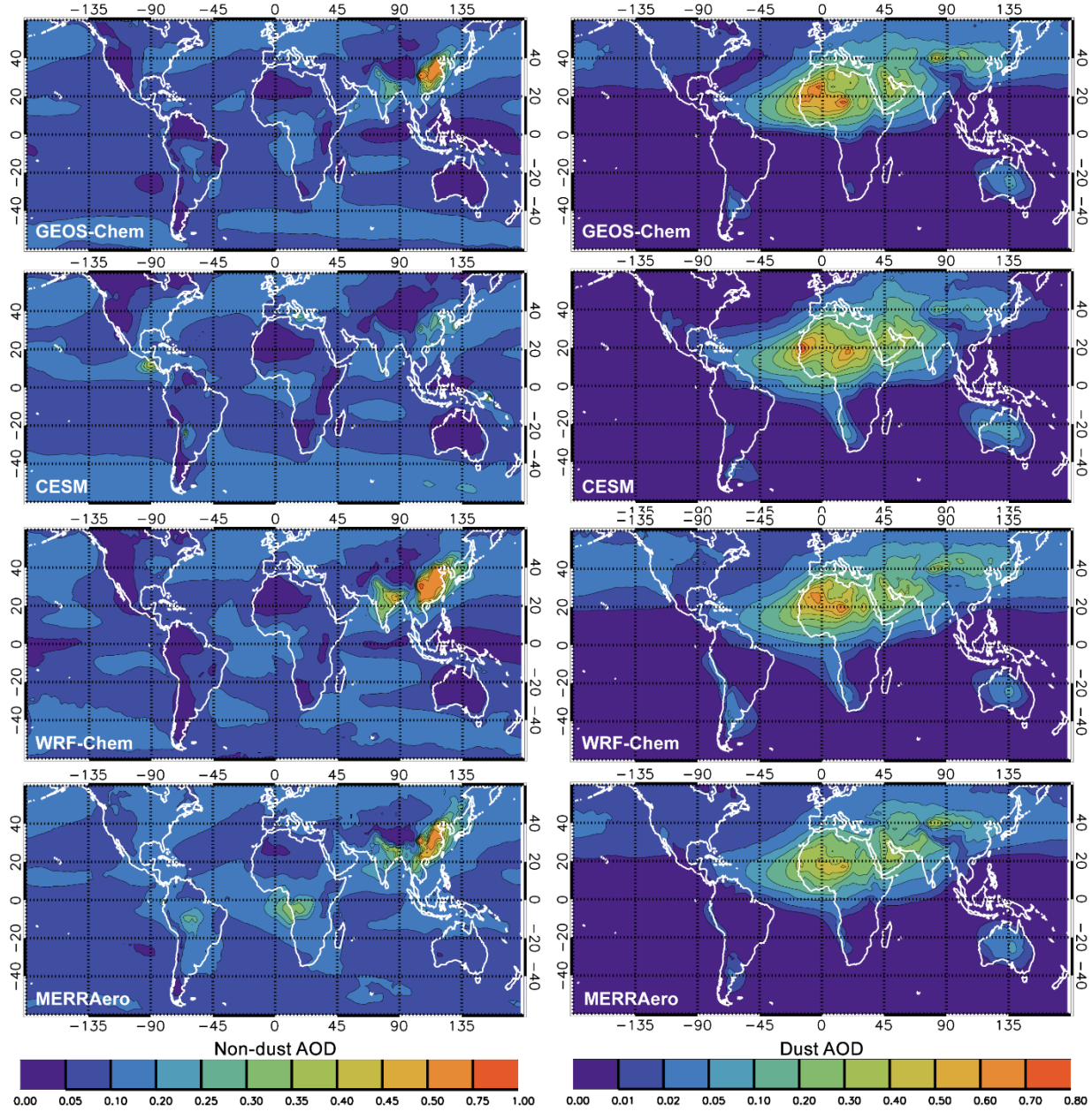

Figure 3 – Annual non-dust AOD (left) and dust AOD (right) at 550 nm for the four models used in this study. Data is averaged over 2004 – 2008.

Atmos. Chem. Phys. Discuss., doi:10.5194/acp-2016-385, 2016
Manuscript under review for journal Atmos. Chem. Phys.
Published: 20 May 2016

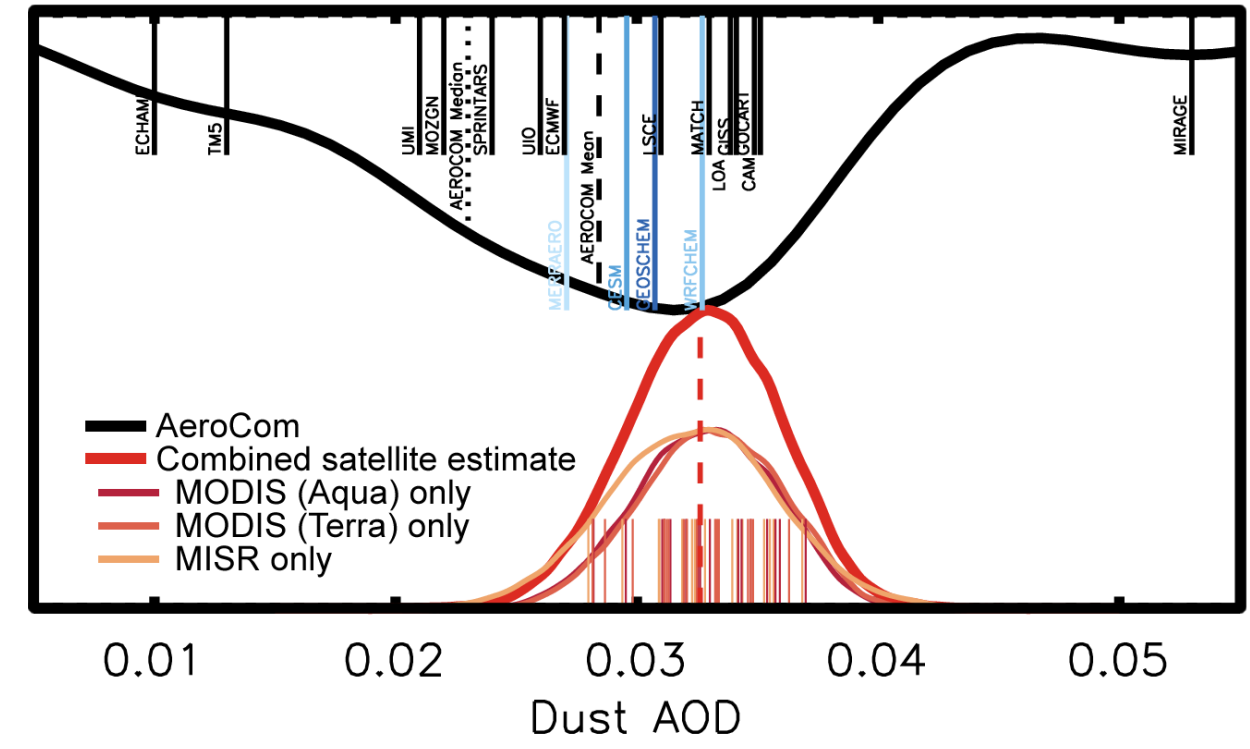

Figure 4 – The global dust AOD adapted from Huneeus et al. (2011) for 14 AeroCom models (vertical black lines) and the associated PDF (solid black line), mean (dashed black line) and the AeroCom median model (dotted black line) are shown along with the global dust AOD from the four models used in this study (vertical blue lines). The PDF of the observationally-constrained dust AOD estimate of this study (red) with the associated mean (dashed red line) is shown on the bottom axis. The PDF of the observationally-constrained dust AOD derived from each of the satellite instruments is shown (red hues) with the individual ensemble members (vertical red hue lines).

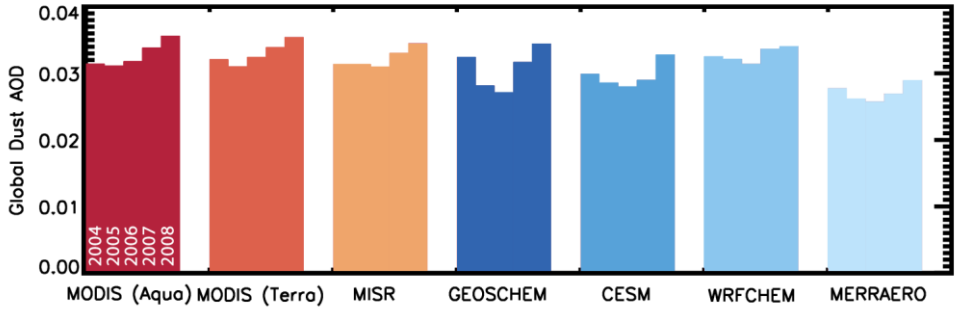

Figure 5 – Annual global dust AOD for 2004 – 2008 derived from the three satellite instruments (red hues) and from the four models (blue hues). The annual dust AOD from the satellite instruments is an average of the ensemble members for that instrument.

Atmos. Chem. Phys. Discuss., doi:10.5194/acp-2016-385, 2016
Manuscript under review for journal Atmos. Chem. Phys.
Published: 20 May 2016

Atmospheric Chemistry and Physics Discussions

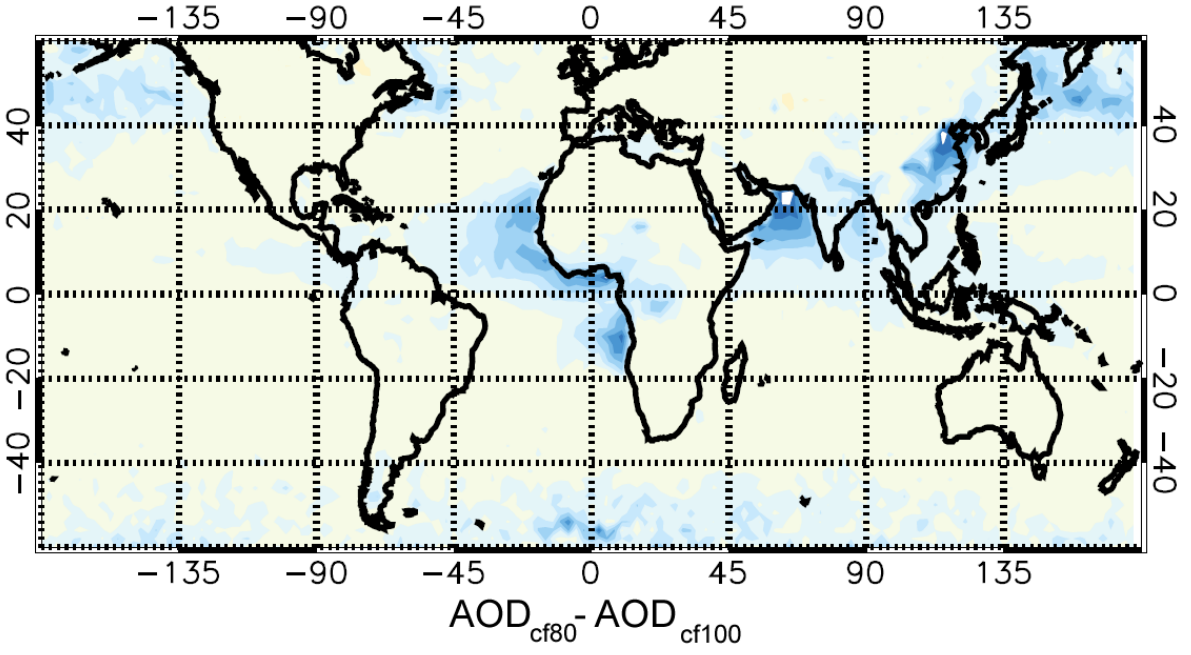

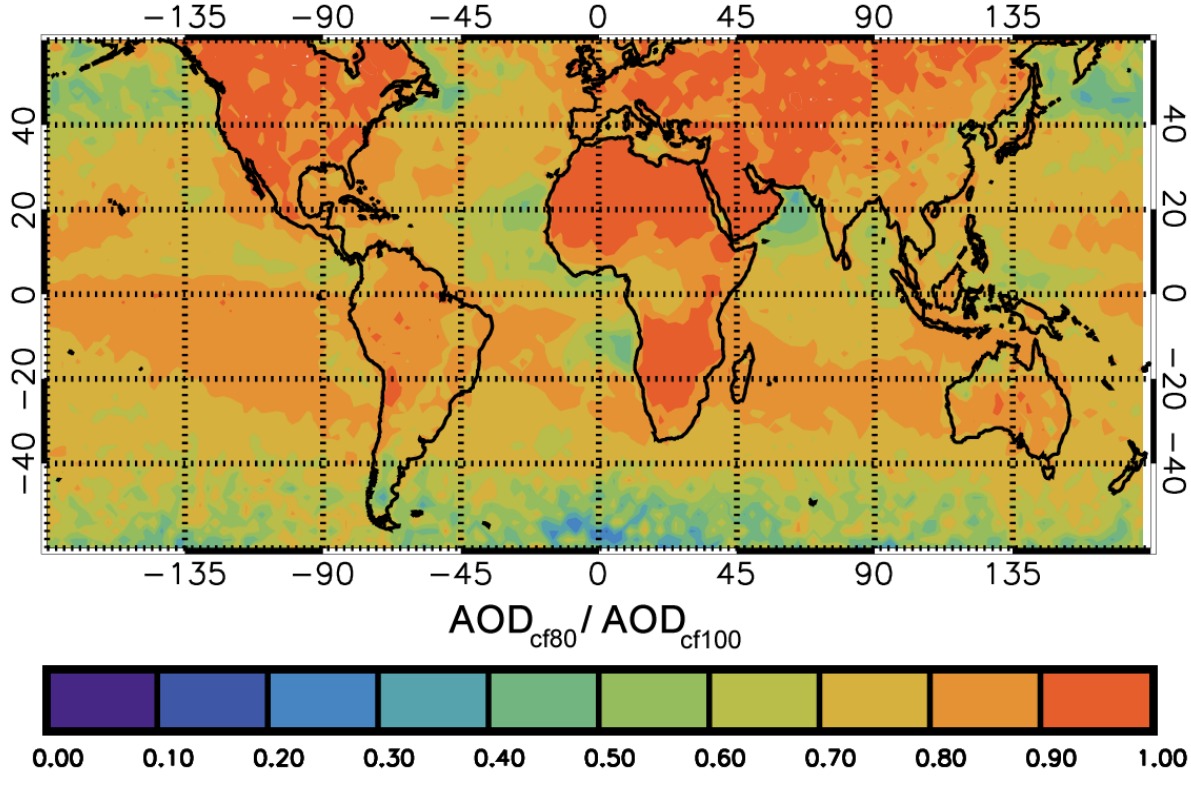

Atmos. Chem. Phys. Discuss., doi:10.5194/acp-2016-385, 2016
Manuscript under review for journal Atmos. Chem. Phys.
Published: 20 May 2016

Atmospheric Chemistry and Physics Discussions

Figure 6 – The absolute change (top) and fractional change (bottom) in the annual MODIS Aqua AOD (averaged over 004 - 2008) when applying a filter to remove any Level-3 data that contains more than 80% cloudy Level-2 pixels.

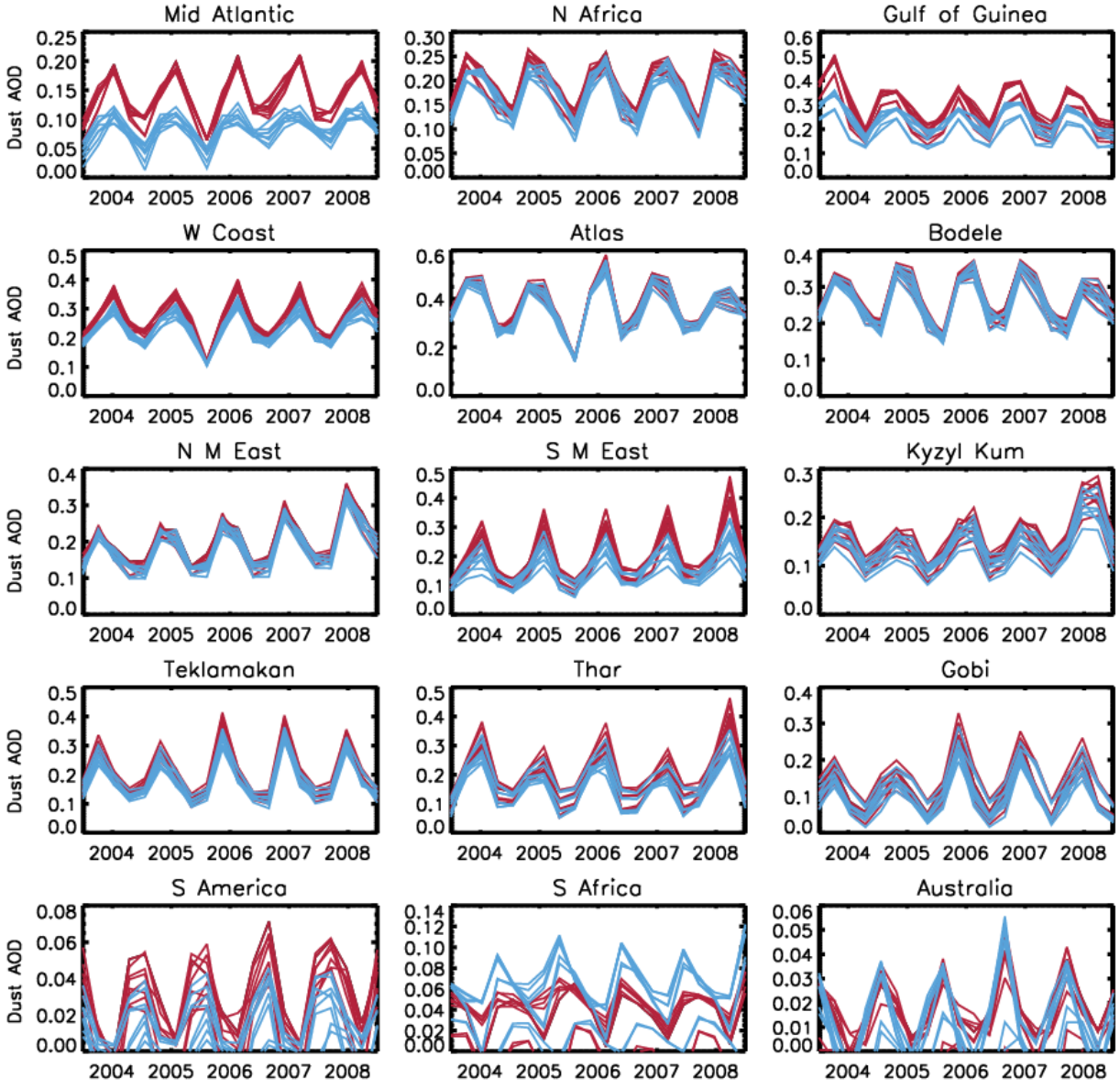

Figure 7 – Observational dust AOD from MODIS Aqua and Terra with (red) and without (blue) filtering of 1° x 1° daily regions with over 80% cloud cover. Each line corresponds to a different combination of satellite and model when calculating the dust AOD, indicating the uncertainty.

Atmos. Chem. Phys. Discuss., doi:10.5194/acp-2016-385, 2016
Manuscript under review for journal Atmos. Chem. Phys.
Published: 20 May 2016

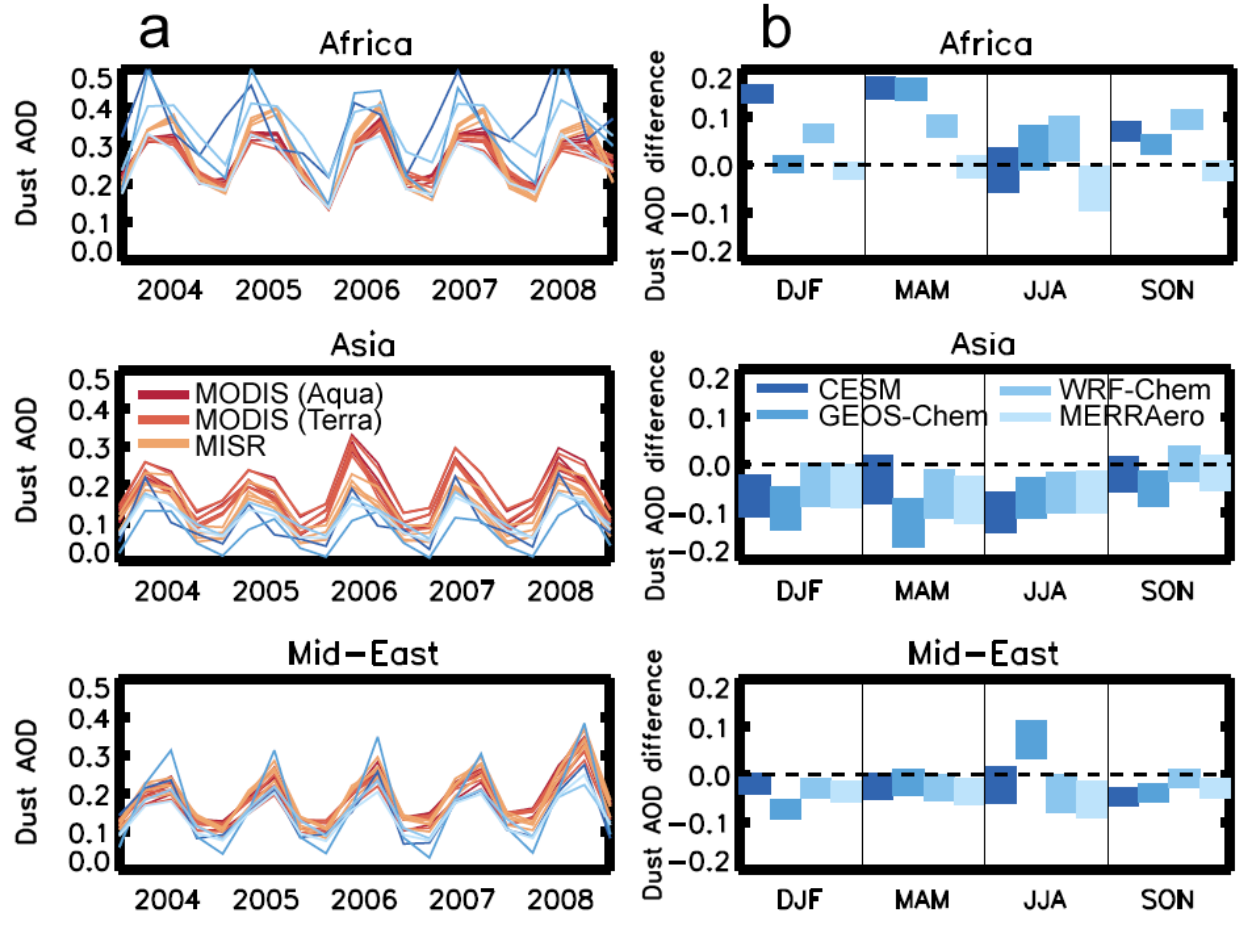

Figure 8 – (a) Seasonal dust AOD between 2004 and 2008 for observational-based estimates (red hues; each of the 12 lines represents a different ensemble member) and for the models (blue hues). (b) To isolate the seasonality, the difference between model and observational-based seasonal dust AOD, averaged over 2004-2008, is shown. Bar thickness indicates the range of the observational-based estimates for each season, deviation from zero (dashed line) indicates the bias in model seasonal dust AOD relative to the observations. The regions are based on area-weighted averages over the subset of regions defined in Figure 1, except Africa, which does not include the Mid-Atlantic region (shown separately in Figure 8 and 9 with other sub-regions).

Atmos. Chem. Phys. Discuss., doi:10.5194/acp-2016-385, 2016
Manuscript under review for journal Atmos. Chem. Phys.
Published: 20 May 2016

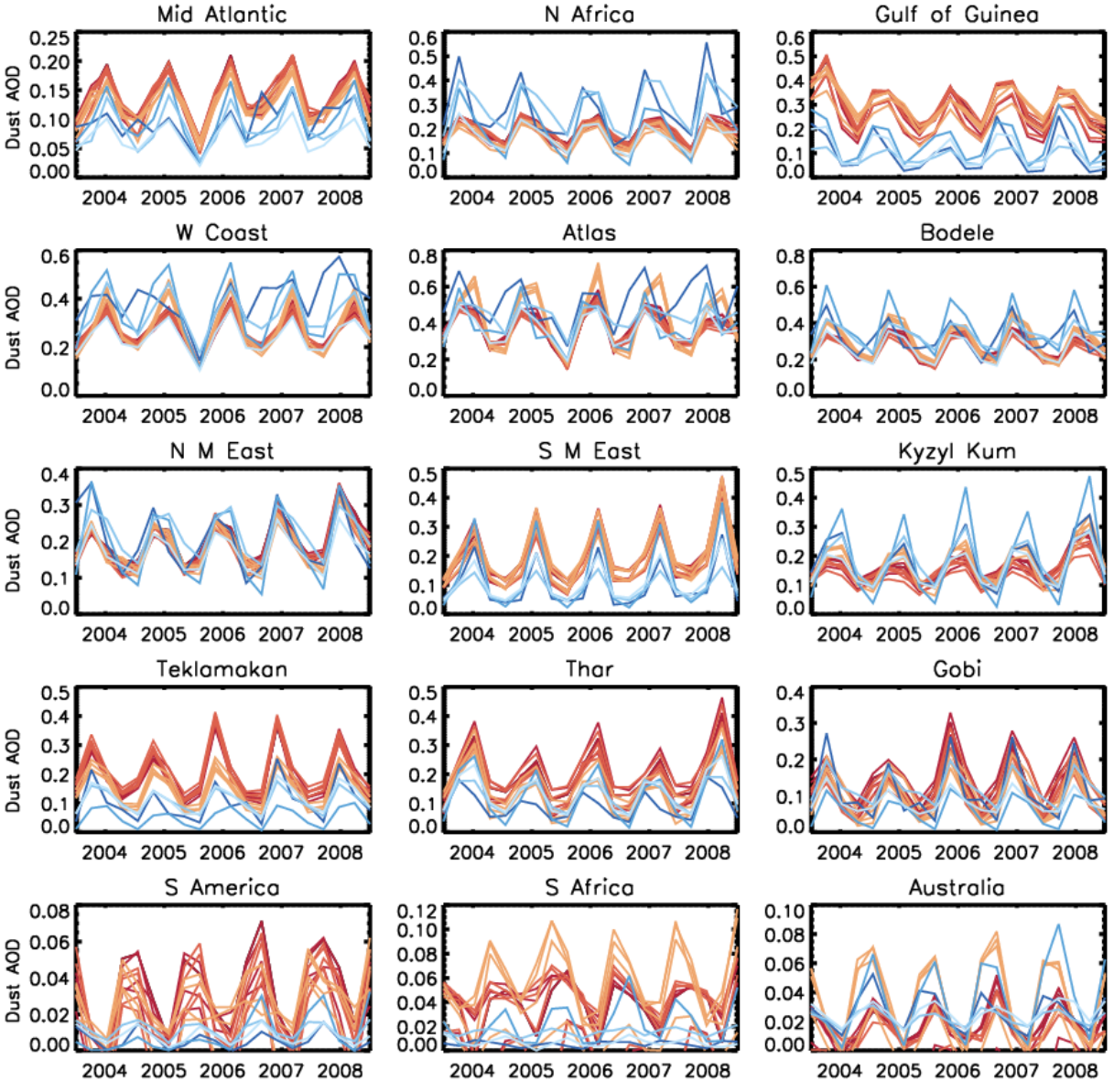

Figure 9 – Same as Figure 8a but for each individual region (in Figure 1). Observational dust AOD is shown for multiple realizations of MODIS Aqua, MODIS Terra and MISR (dark to light red). Models are GEOS-Chem, CESM, WRF-Chem and MERRAero (dark to light blue).

Atmos. Chem. Phys. Discuss., doi:10.5194/acp-2016-385, 2016
Manuscript under review for journal Atmos. Chem. Phys.
Published: 20 May 2016

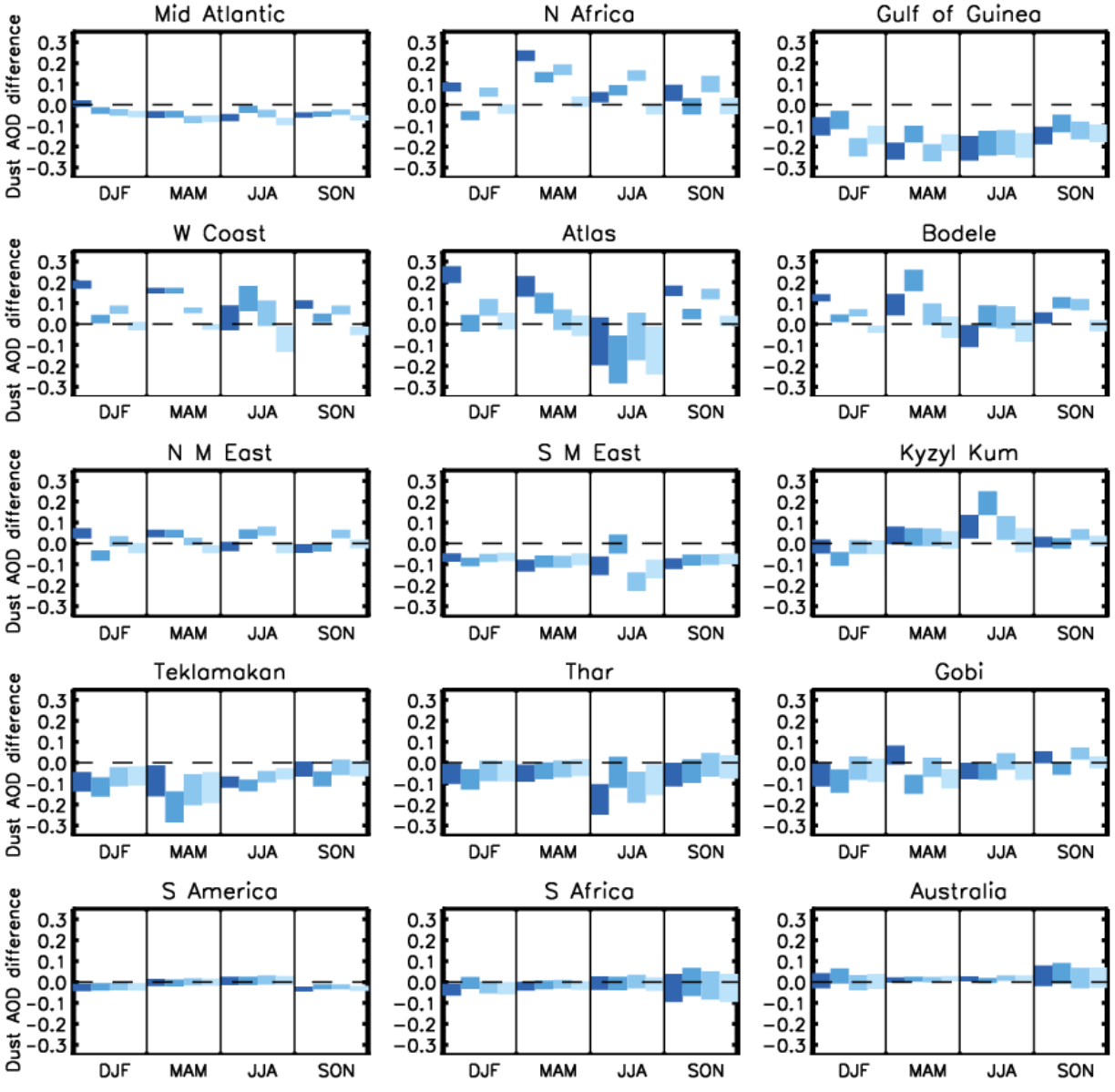

Figure 10 – same as Figure 8b but for individual regions (in Figure 1). Models are GEOS-Chem, CESM, WRF-Chem and MERRAero (dark to light blue).